

RESEARCH ARTICLE

A stress-response-related inter-compartmental signalling pathway regulates embryonic cuticle integrity in Arabidopsis

Audrey Creff¹, Lysiane Brocard², Jérôme Joubès³, Ludivine Taconnat⁴, Nicolas M. Doll¹, Anne-Charlotte Marsollier¹, Stéphanie Pascal⁵, Roberta Galletti¹, Sophy Boeuf¹, Steven Moussu¹, Thomas Widiez¹, Frédéric Domergue^{5*}, Gwyneth Ingram^{1*}

1 Laboratoire Reproduction et Développement des Plantes, Univ Lyon, ENS de Lyon, CNRS, INRA, Lyon, France, **2** Pôle d'Imagerie du Végétal, UMS3420-Université de Bordeaux, CNRS, INSERM, Domaine de la Grande Ferrade, Villenave d'Ornon, France, **3** Laboratoire de Biogenèse Membranaire, UMR 5200 Université de Bordeaux, Villenave d'Ornon, France, **4** Institut of Plant Sciences Paris-Saclay (IPS2), UMR 9213/UMR1403, CNRS, INRA, Université Paris-Sud, Université d'Evry, Université Paris-Diderot, Sorbonne Paris-Cité, Orsay, France, **5** Laboratoire de Biogenèse Membranaire, UMR 5200 CNRS, Villenave d'Ornon, France

* Frederic.Domergue@u-bordeaux.fr (FD); Gwyneth.Ingram@ens-lyon.fr (GI)



OPEN ACCESS

Citation: Creff A, Brocard L, Joubès J, Taconnat L, Doll NM, Marsollier A-C, et al. (2019) A stress-response-related inter-compartmental signalling pathway regulates embryonic cuticle integrity in Arabidopsis. PLoS Genet 15(4): e1007847. <https://doi.org/10.1371/journal.pgen.1007847>

Editor: Claudia Köhler, Swedish University of Agricultural Sciences (SLU), SWEDEN

Received: November 20, 2018

Accepted: March 7, 2019

Published: April 18, 2019

Copyright: © 2019 Creff et al. This is an open access article distributed under the terms of the [Creative Commons Attribution License](https://creativecommons.org/licenses/by/4.0/), which permits unrestricted use, distribution, and reproduction in any medium, provided the original author and source are credited.

Data Availability Statement: Microarray data from this article were deposited at Gene Expression Omnibus (<http://www.ncbi.nlm.nih.gov/geo/>), accession no. GSE68048) and at CATdb (http://tools.ips2.u-psud.fr/cgi-bin/projects/CATdb/consult_project.pl?project_id=383) according to the "Minimum Information About a Microarray Experiment" standards.

Funding: "AC was funded by a grant from the French National Research Agency (ANR) (ANR-13-BSV2-0002, INASEED). SM was supported by a

Abstract

The embryonic cuticle is necessary for normal seed development and seedling establishment in Arabidopsis. Although mutants with defective embryonic cuticles have been identified, neither the deposition of cuticle material, nor its regulation, has been described during embryogenesis. Here we use electron microscopy, cuticle staining and permeability assays to show that cuticle deposition initiates *de novo* in patches on globular embryos. By combining these techniques with genetics and gene expression analysis, we show that successful patch coalescence to form a continuous cuticle requires a signalling involving the endosperm-specific subtilisin protease ALE1 and the receptor kinases GSO1 and GSO2, which are expressed in the developing embryonic epidermis. Transcriptome analysis shows that this pathway regulates stress-related gene expression in seeds. Consistent with these findings we show genetically, and through activity analysis, that the stress-associated MPK6 protein acts downstream of GSO1 and GSO2 in the developing embryo. We propose that a stress-related signalling pathway has been hijacked in some angiosperm seeds through the recruitment of endosperm-specific components. Our work reveals the presence of an inter-compartmental dialogue between the endosperm and embryo that ensures the formation of an intact and functional cuticle around the developing embryo through an "auto-immune" type interaction.

Author summary

Plant embryogenesis occurs deep within the tissues of the developing seed, and leads to the production of the mature embryo. In Arabidopsis and many other plant species embryo-derive structure (such as the cotyledons) are suddenly exposed to environmental

doctoral grant from the Région Auvergne-Rhône-Alpes. RG was supported by a European Research Council (ERC) Starting Grant (Phymorph #307387). NMD was supported by a PhD fellowship from the Ministère de l'Enseignement Supérieur, de la Recherche Scientifique et des Technologies de l'Information et de la Communication. Microscopy and lipid analyses were respectively performed at the Bordeaux Imaging Center (which is a member of the national infrastructure France BioImaging), and the Metabolome Facility of the Functional Genomic Center of Bordeaux (which is supported by the CNRS: MetaboHUB-ANR-11-INBS-0010). The funders had no role in study design, data collection and analysis, decision to publish, or preparation of the manuscript."

Competing interests: The authors have declared that no competing interests exist.

stresses such as low humidity. In these species the embryonic cuticle provides a primary defence against environmental stress, and particularly dehydration, at germination. The formation of an intact and functional cuticle during embryogenesis is thus of key importance for seedling survival. Our work shows that a signalling pathway involving receptor-kinases expressed in the embryo epidermis, and a protease expressed in the endosperm tissue surrounding the embryo, is critical for ensuring the production of an intact cuticle. Furthermore, we show that a component of stress-related MAP-Kinase signalling in plants acts downstream in this pathway, possibly to mediate transcriptional responses characteristic of responses to stress. We propose that plants have redeployed a signalling pathway associated with stress resistance to ensure the formation of an intact embryonic cuticle prior to germination, and thus ensure seedling survival at germination.

Introduction

The Arabidopsis seed is a complex structure composed of three genetically distinct compartments, the maternally-derived seed coat, the embryo, and the endosperm. After fertilization the expansion of the endosperm drives the growth of the seed. However, during later developmental stages the endosperm breaks down, leaving space for the growing embryo. By the end of seed development, only a single endosperm cell layer envelops the embryonic tissues (reviewed in [1]).

The endosperm is an angiosperm innovation, thought to have arisen through the sexualisation of the central cell of the female gametophyte [2]. The ancestors of angiosperms probably had seeds more similar to those of gymnosperms, in which tissues of the female gametophyte proliferate independently of egg cell fertilization to produce a nutrient rich storage tissue. However, the endosperm plays not only a nutritional role, but also a role in regulating embryo development. For example, the peptide CLAVATA3/EMBRYO SURROUNDING REGION--RELATED8 (CLE8) may act non-cell autonomously to regulate early Arabidopsis embryogenesis [3]. Recently, maternally-expressed peptides present in the central cell pre-fertilization, and subsequently in the early EMBRYO SURROUNDING REGION (ESR), were shown to regulate Arabidopsis suspensor development. Genetic analysis suggests that this regulation could be mediated by a pathway involving the Receptor-Like Cytoplasmic Kinase SHORT SUSPENSOR [4,5], although the receptor involved remains unidentified.

In previous work we showed genetically that the ESR-specific subtilisin protease Abnormal LEaf-shape1 (ALE1) acts in the same genetic pathway as two embryonically-expressed receptor kinases, GASSHO1 [(GSO1) also known as SCHENGEN3 [6]] and GASSHO2 (GSO2), to control the formation of the embryonic cuticle in developing seeds [7–10]. Our results indicate that a seed specific inter-tissue signalling event is necessary for the formation of a functional embryonic cuticle [7]. The results of genetic studies have led us to speculate that the role of this pathway is to ensure the robust elimination of apoplastic continuity between the developing embryo and the surrounding endosperm thus gating molecular movement between the two compartments [11,12].

The cuticle is the outermost layer of the aerial parts of the plant. It is a highly complex structure mainly composed of a lipid polymer (cutin) and waxes, either associated with the polymer (intracuticular waxes) or deposited on the top of it (epicuticular waxes) (recently reviewed in [13,14]). Cutin and waxes are composed of complex mixtures of hydroxylated and very long-chain fatty acid derivatives, respectively. Cuticle structure and composition are highly regulated not only at the tissue level, but also in response to environmental stimuli such as drought, radiation and pollution [13,14]. In addition, several reports have highlighted the important

role played by the cuticle in biotic interactions, and particularly in protecting plants from attack by bacterial pathogens (reviewed in [13,15,16]).

In Arabidopsis although little, if any, evidence exists for the presence of cutin-like substances in the wall between the mature egg cell and the central cell, by the end of embryogenesis the hypocotyl and cotyledons of the embryo are covered with a continuous cuticle which renders the germinating seedling impermeable to hydrophilic dyes, and resistant to water loss [17]. Cuticle biogenesis is considered to be a unique property of epidermal cells [18]. During plant development, epidermal cells are generated by anticlinal divisions of pre-existing epidermal cells so that each cell inherits an intact external cuticularised cell wall. In this respect the embryonic cuticle is atypical as it is deposited *de novo* at the interface between the developing embryo and endosperm. Although mutants with defective embryonic cuticles have been described [7–10,17], only very fragmentary evidence about when the embryonic cuticle appears is present in the literature. Furthermore, the structure of the embryonic cuticle, its composition, the mechanisms via which it is deposited and its function during seed development remain unexplored. In this study we aimed to elucidate how the embryonic cuticle is formed, and to investigate how the ALE1 GSO1 GSO2 signalling pathway impacts its biosynthesis and deposition.

Results

Expression of genes involved in cuticle deposition initiates during early embryogenesis

An inspection of available *in silico* data [19–21] showed that many genes encoding enzymes thought to be involved in cutin biosynthesis are expressed during early embryogenesis (S1 Fig). *In situ* hybridisations confirmed that genes known to affect cuticle production (*LACS2* [22,23], *FIDDLEHEAD/KCS10* [24–27], *LACERATA* [28] and *BODYGUARD* [29]) or export (*LTPG1* [30] and *ABCG11* [31]) have a clear epidermis-specific expression from the mid globular stage onwards (Fig 1, S3 Fig, S3 Fig).

In agreement with published and *in silico* data [9] (S1 Fig) *GSO1* and *GSO2* were expressed in the embryo from early developmental stages (Fig 1, S3 Fig). In addition, their expression was mainly restricted to the embryonic epidermis. *GSO1* expression in the embryonic epidermis was further confirmed using plants expressing a functional genomic *GSO1*-*mVENUS* fusion under the control of the *GSO1* promoter (*pGSO1:GSO1-mVENUS*) [6] (Fig 2). This construction fully complemented the cuticle permeability phenotype of *gso1-1 gso2-1* double mutant seedlings, and strongly reduced the misshapen-seed phenotype of *gso1-1 gso2-1* mutant seeds when introduced into the *gso1-1 gso2-1* mutant background (Fig 2).

Since previous results showed that epidermal identity is not affected in *gso1-1 gso2-1* mutants [12], the expression of cuticle biosynthesis genes was analysed by *in situ* hybridization in *gso1-1 gso2-1* double mutant seeds (which show a stronger cuticle phenotype than *ale1-4* mutants [7]). As shown in Fig 1 (and S2 Fig and S3 Fig), no reduction in the expression of any of the cuticle biogenesis genes analysed was detected in the embryonic epidermis of this background, whereas reduced expression of both *GSO1* and *GSO2* was clearly visible. For these results, we concluded that although many genes involved in cuticle biosynthesis are co-expressed with *GSO1* and *GSO2* in the embryonic epidermis, their expression is not dependent upon *GSO1* and *GSO2*.

Loss of *GSO1/GSO2* and *ALE1* function affects cuticle integrity

The cutin content of seedling cotyledons was assessed by measuring the quantities of the main cutin monomers released after cutin isolation followed by depolymerisation (mainly C16 and

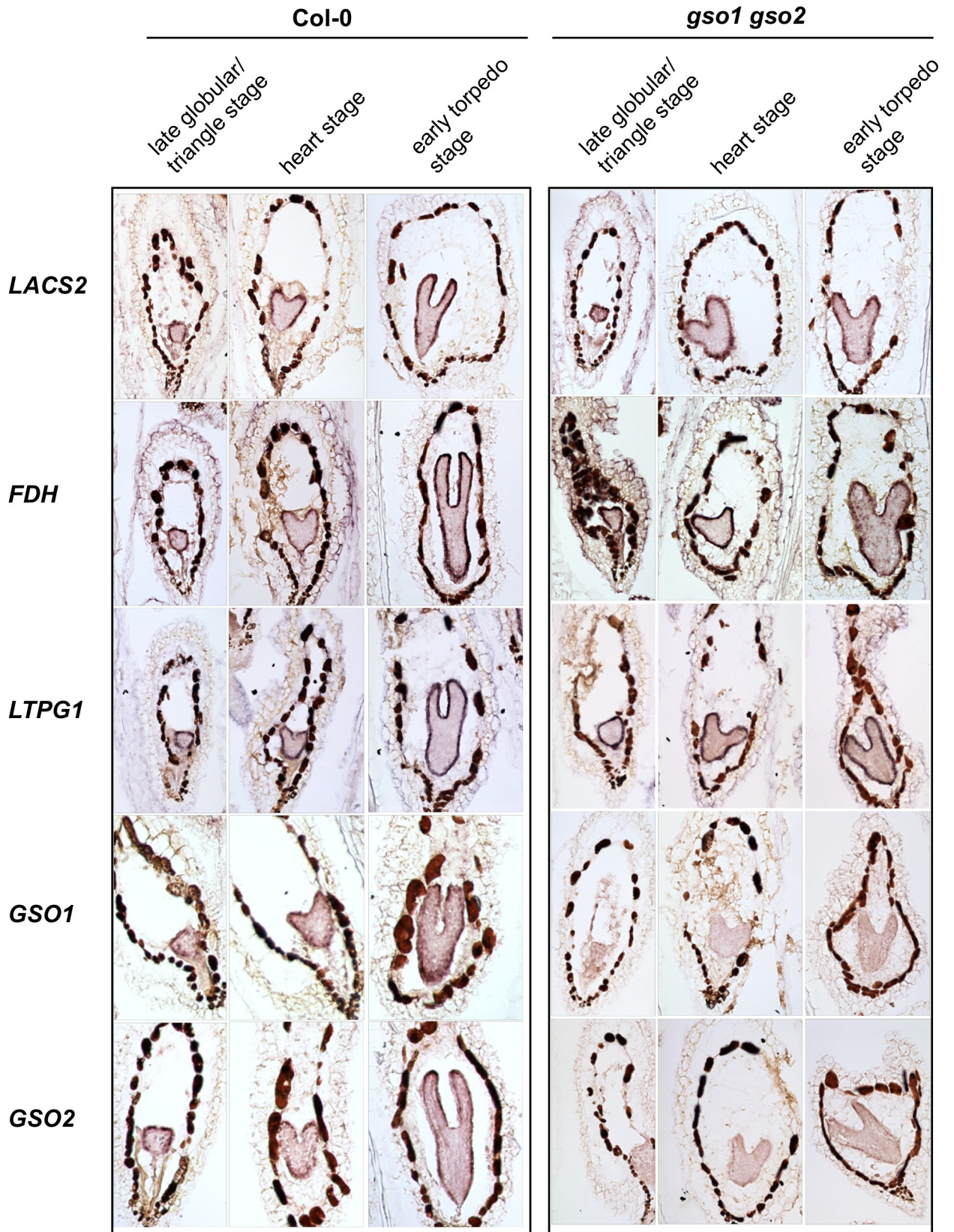


Fig 1. Genes involved in cuticle biosynthesis are co-expressed with GSO1 and GSO2 during embryogenesis, but their expression is not dependent upon GSO1 and GSO2. Analysis of the expression of genes involved in cuticle biosynthesis in wild-type (Col-0) and *gso1-1 gso2-1* seeds containing late globular/triangle, heart and early torpedo stage embryos (left to right).

<https://doi.org/10.1371/journal.pgen.1007847.g001>

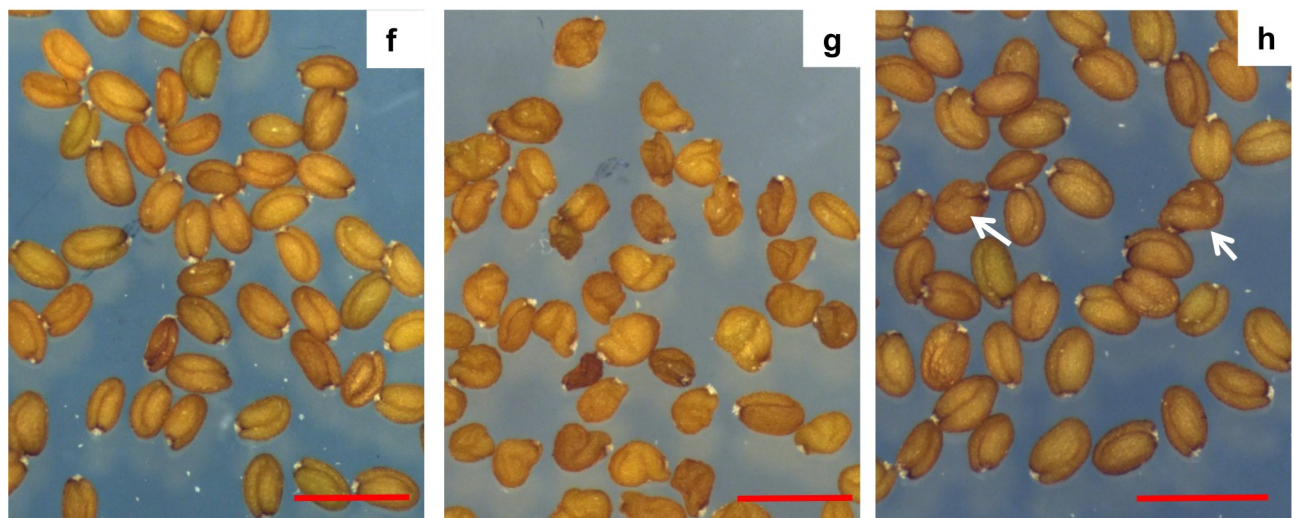
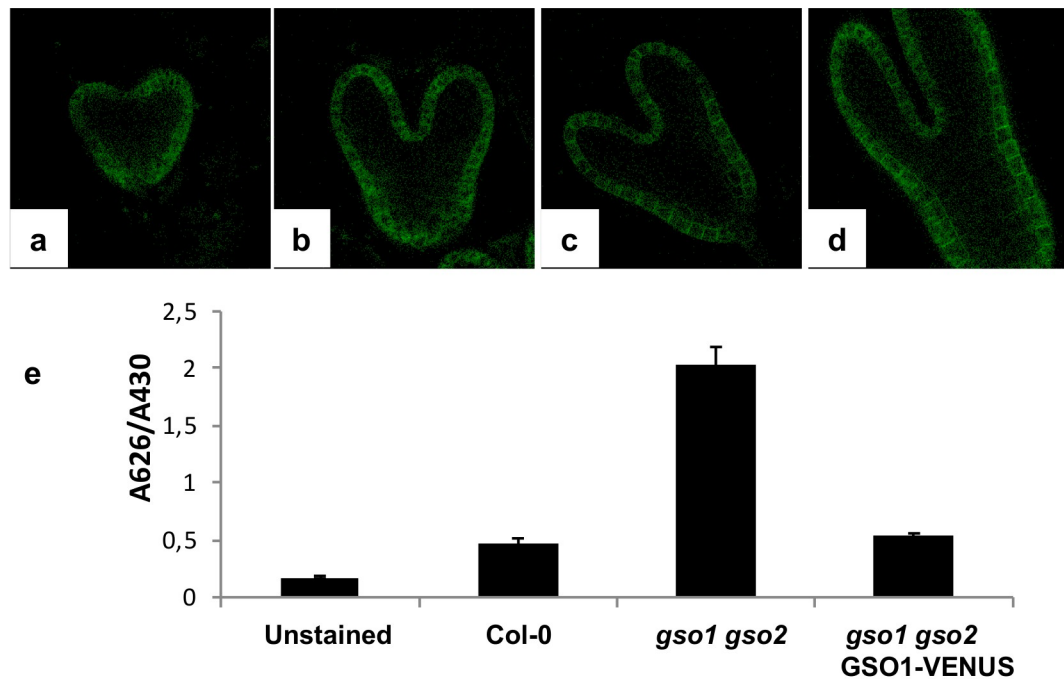


Fig 2. Localisation and functionality of the *pGSO1:GSO1-mVENUS* transgene in developing embryos. Confocal images of GSO1-mVENUS at early heart, mid heart, late heart and early torpedo stages of development (a-d). (e) The *pGSO1:GSO1-mVENUS* transgene complements seedling cuticle defects in *gso1-1 gso2-1* double mutants. Quantification of seedling toluidine blue permeability was carried out as described in Moussu et al., 2017. Error bars represent standard errors from three biological replicates. (f-h) The *pGSO1:GSO1-mVENUS* transgene complements seed shape defects in *gso1-1 gso2-1* double mutants. Seed populations from wild-type (f), *gso1-1 gso2-1* double mutants (g) and *gso1-1 gso2-1* double mutants carrying the *pGSO1:GSO1-mVENUS* transgene (h). Occasional misshapen shaped seeds are observed in the complemented line (white arrows), compared with nearly 100% misshapen seeds in the un-complemented double mutant. Scale bar = 1mm.

<https://doi.org/10.1371/journal.pgen.1007847.g002>

C18 ω OH (omega-hydroxy acid) and DCA (α,ω -dicarboxylic acid)). As clearly illustrated by the quantification of 18:2-DCA, the major component of Arabidopsis cutin, a slight loss in cutin load was detected in *gso1-1 gso2-1*, but not in *ale1-4* cotyledons compared to wild-type. In contrast a very clear reduction in cutin load was observed in control plants lacking the acyl-transferases GPAT4 and GPAT8 required for cutin biosynthesis, as has previously been reported in rosette leaves [32] (Fig 3A). We therefore investigated the cuticle permeability of etiolated cotyledons by submerging them in the hydrophilic dye toluidine blue, which can only penetrate internal tissues through defects in the cuticle [17]. Surprisingly, we found that the cotyledons of etiolated *gpat4 gpat8* seedlings showed a rather similar toluidine blue permeability to *ale1-4* seedlings and a considerably reduced permeability compared to *gso1-1 gso1-2* double mutants, suggesting that the *gpat4 gpat8* cuticle, although quantitatively strongly deficient in cutin monomers, remains partially functional (Fig 3B). Taken together with gene expression analysis, these results suggest that the ALE1, GSO1 and GSO2-mediated signalling pathway might impact cuticle organisation or integrity rather than the quantity of cuticle components produced by epidermal cells.

The process of embryonic cuticle deposition was investigated in more detail in wild-type (Col-0) seeds (Fig 4A–4D). At the two-cell stage the embryo was surrounded by a thick cell wall but no electron dense material was detected at the embryo surface. At the mid-late globular stage, a cutin-like electron-dense material was detected in patches (Fig 4B and S4 Fig). From heart stage onwards, an apparently continuous layer of electron-dense cutin-like material was detected at the surface of the outer epidermal cell wall. Embryonic cuticle production therefore involves the *de novo* deposition and subsequent coalescence of “patches” of cuticular material at the surface of epidermal cells. Toluidine blue assays with wild-type embryos extruded at different developmental stages indicated that embryonic cuticle permeability started to reduce noticeably at the mid torpedo stage (after apparent gap closure), and that the embryo cuticle continues to become more and more impermeable during embryo development (S5 Fig). These results suggest that the coalescence of visible gaps in the embryonic cuticle precedes a measurable reduction in embryonic permeability, and that cuticle reinforcement continues throughout embryogenesis.

In *gso1-1 gso2-1* mutant embryos the cuticle still showed discontinuities at the heart and walking stick stage (Fig 4E and 4F, S4 Fig). In this background the cuticle also appeared thicker, but less condensed than that of wild-type embryos. The outer epidermal cell wall was also abnormally thick at later stages (compare embryonic cell wall thickness in Fig 4D with that in 4F). Similar discontinuities were observed, although at a lower frequency, in the *ale1-4* background at the heart stage as described previously [10], but were less frequent at later stages, consistent with the less severe cuticle permeability phenotype observed in the seedlings of this background (Fig 4G and 4H). Consistent with these observations *ale1* and *gso1-1 gso2-1* mutant embryos remained permeable to toluidine blue throughout embryogenesis (Fig 5), with permeability phenotypes in fully expanded but immature embryos correlating closely with those observed in etiolated seedlings. Importantly *ale1* mutants were more permeable to toluidine blue at embryo maturity despite an apparent lack of visible gaps in the *ale1* cuticle after the torpedo stage. Interestingly fully expanded embryos of *gpat4 gpat8* mutants were not significantly more permeable than those of wild-type plants, suggesting that permeability defects observed in etiolated seedlings in this background could be due to the rapid expansion of embryonic tissues (especially the hypocotyl) after germination. These results are consistent with our hypothesis that the ALE1 GSO1 GSO2 pathway is necessary for generating a continuous cuticle layer and further suggest that it controls “gap closure” during embryonic cuticle maturation.

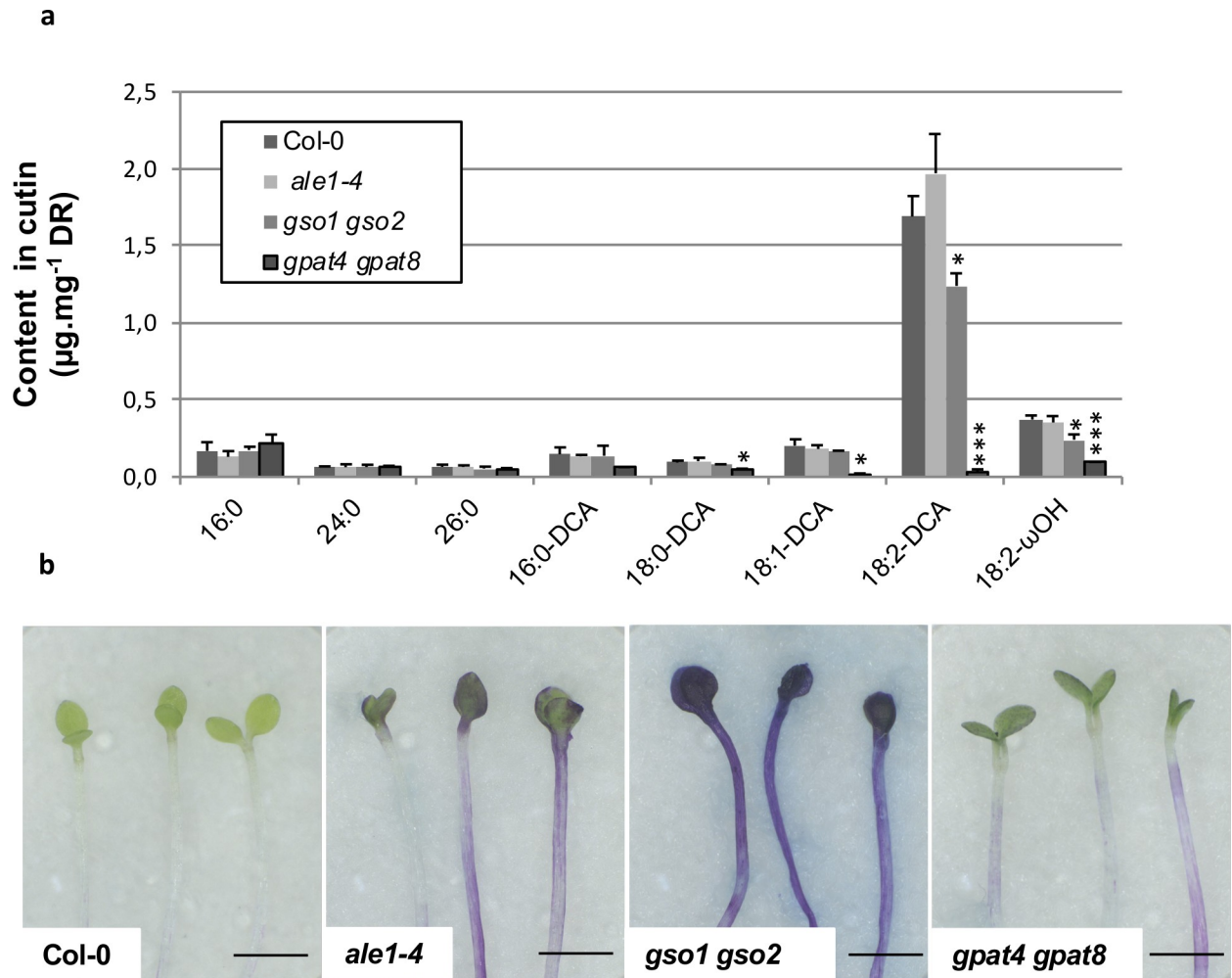


Fig 3. Cuticle permeability defects in *ale1-4* and *gso1-1 gso2-1* seedlings do not correlate with changes in cutin load. (a) Cotyledons grown *in vitro* for 5 days under continuous light were collected, delipidated and their cutin content and composition was analyzed as described in the Material and Method section. ωOH and DCA stand respectively for omega-hydroxy acid and α,ω-dicarboxylic acid. Mean values are shown in µg/mg of delipidated dry residue (DR) ± SD of three replicates. Statistical differences were determined according to a Student's *t* test: *** denotes $p < 0.0001$, ** denotes $p < 0.001$ and * denotes $p < 0.01$. (b) Cuticle permeability to toluidine blue in etiolated seedlings from the genotypes tested in (a).

<https://doi.org/10.1371/journal.pgen.1007847.g003>

GSO1 GSO2 and ALE1 regulate overlapping gene sets and promote the expression of defence related genes during seed development

Transcriptional analysis of intact siliques from *gso1-1 gso2-1* and *ale1-4* mutants and wild-type plants was carried out at globular and heart stages. The results are provided in Fig 6A and 6B, S1 Table, S6 Fig and S7 Fig. The number of differentially down-regulated genes in the mutant backgrounds compared to wild-type was higher than the number of up-regulated genes (S1 Table). A moderate overlap between genes showing higher expression in *ale1-4* and *gso1-1 gso2-1* mutants than wild-type controls was observed (S6 Fig, S1 Table). In contrast more than three quarters of the genes showing reduced expression at both developmental stages in the *gso1-1 gso2-1* background also showed reduced expression at both developmental stages in *ale1-4* mutants (Fig 6A and S1 Table), corroborating previously published genetic evidence that *ALE1*, *GSO1* and *GSO2* act in the same genetic pathway [7]. Because *ALE1* appears to be

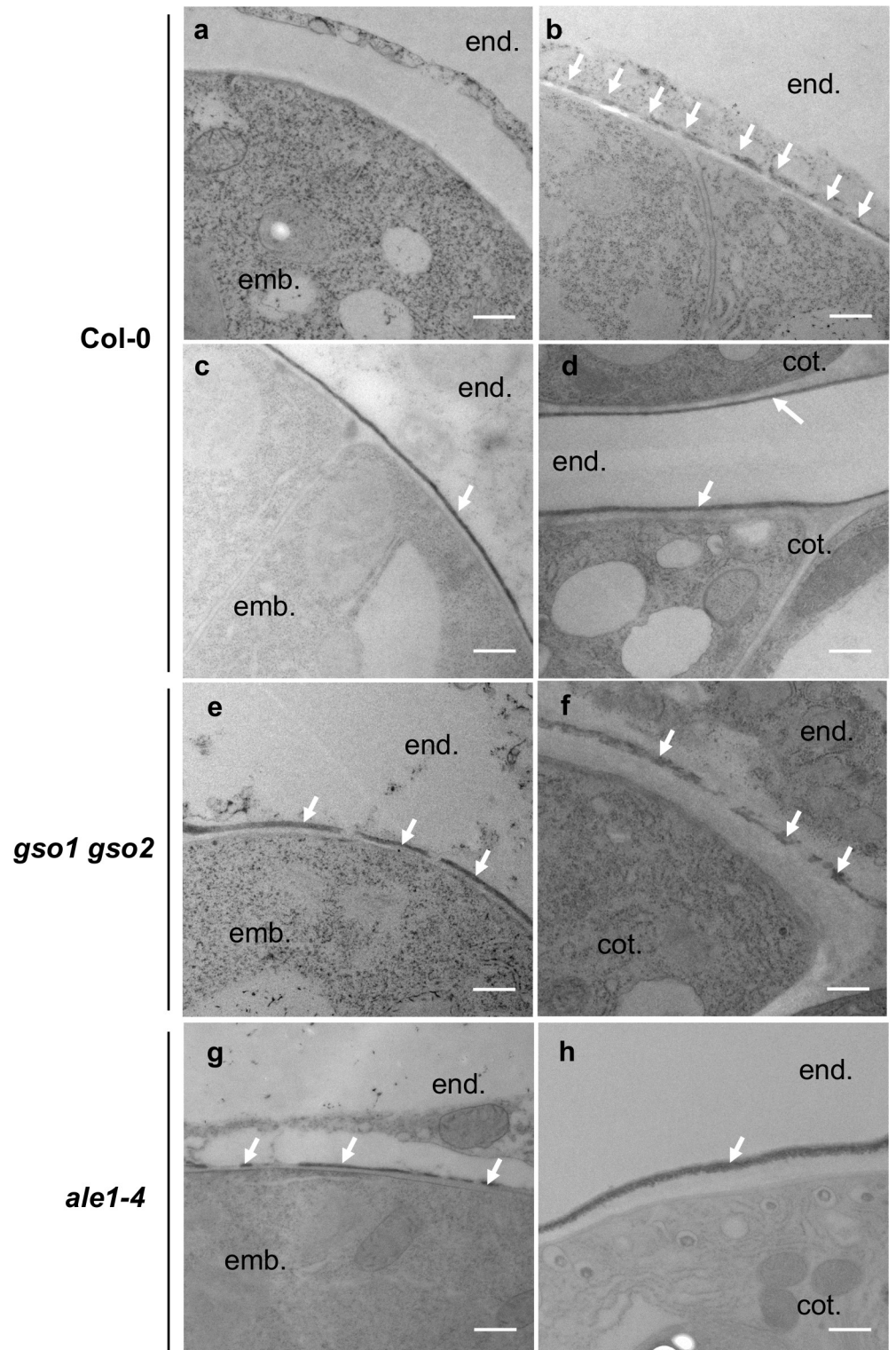


Fig 4. Embryonic cuticle biogenesis involves a process of patch coalescence that is defective in *ale1-4* and *gso1-1 gso2-1* mutants. Analysis of embryonic cuticle deposition in wild-type (a-d), *gso1-1 gso2-1* (e-f) and *ale1-4* (g,h) embryos at 2 cell (a), mid globular (b), mid heart (c,e,g) and walking stick (d,f,h) stages of embryogenesis. White arrows show the external face of the embryonic cuticle. Embryo (emb.), endosperm (end.) and cotyledon (cot.) (for late stages), are labelled. Scale bar = 500nm.

<https://doi.org/10.1371/journal.pgen.1007847.g004>

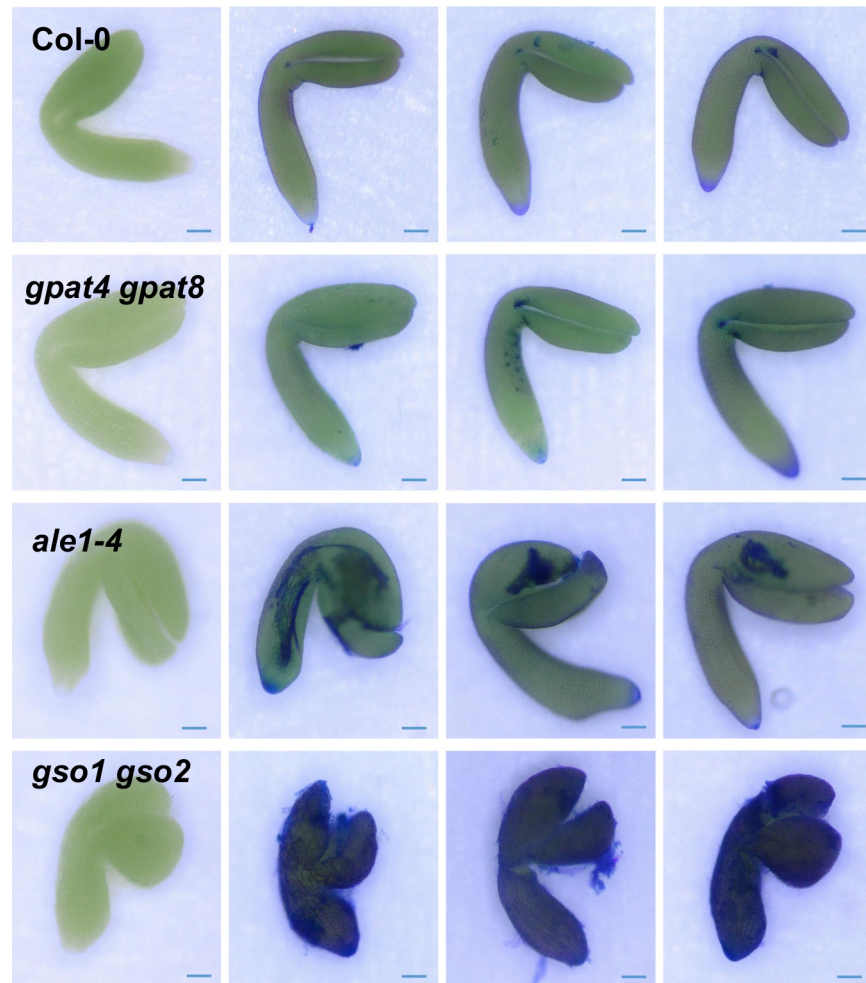


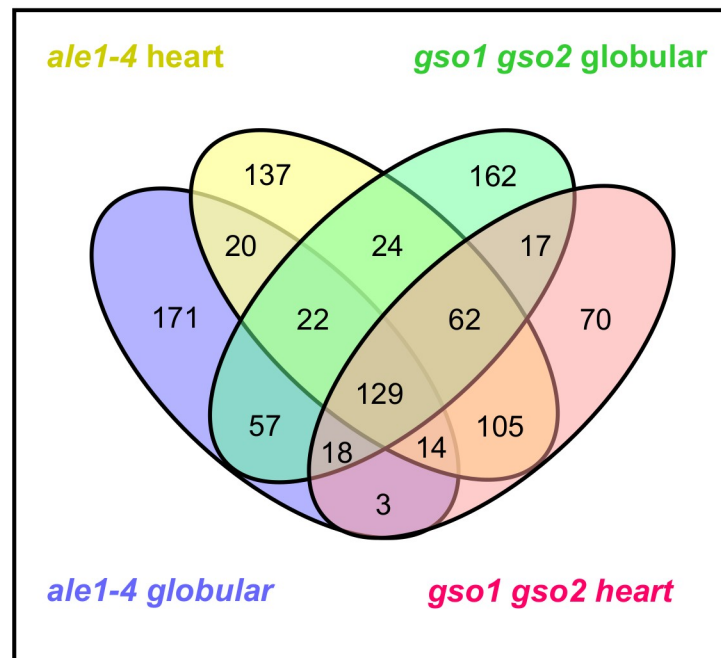
Fig 5. Embryo impermeability phenotypes correspond to seedling impermeability phenotypes in *ale1* and *gso1/gso2* double mutants. Cuticle permeability phenotypes of fully expanded but immature *gpat4 gpat8*, *ale1-4*, and *gso1-1 gso2-1* embryos. Scale bar = 50 μ m. Representative unstained embryos of each genotype are shown in the left-hand column, and a representative sample of stained embryos are shown in the following three columns.

<https://doi.org/10.1371/journal.pgen.1007847.g005>

expressed exclusively in the ESR region of the endosperm [7,8,10], genes mis-regulated in both mutant backgrounds likely comprise *bona fide* targets (direct and indirect) of the ALE1 GSO1 GSO2 pathway, despite the fact that the expression of *GSO1* and *GSO2* is not restricted to the seed [6,9,20].

Genes up-regulated in both mutant backgrounds showed a moderate over-representation in GO terms associated with responses to abiotic stress (S6 Fig). In contrast, genes down-regulated in both backgrounds, particularly at the heart stage, showed a very striking overrepresentation for GO terms linked to abiotic and biotic stress responses (Fig 6B, S7 Fig). Mis-regulation of 19 of these genes was validated using additional independent biological samples by qRT-PCR (S8 Fig). The expression levels of these genes in seeds were generally low, and attempts to carry out *in situ* hybridization were inconclusive. However, for one target, *SWI3A* [33], expression in the developing embryo predicted from *in silico* data was confirmed, and shown to be convincingly reduced in embryos of the *gso1-1 gso2-1* double mutant (S9 Fig). Thus, consistent with the embryonic expression of *GSO1* and *GSO2*, some of the transcriptional regulation downstream of ALE1 GSO1 GSO2 signalling occurs in the embryo.

a



b

Term	p-value
response to chitin	2.58E-26
response to stimulus	3.62E-25
response to carbohydrate stimulus	1.29E-23
response to stress	6.65E-16
response to organic substance	4.69E-15
response to chemical stimulus	7.29E-13
response to wounding	6.71E-11
immune system process	2.42E-10
innate immune response	6.71E-09
immune response	7.81E-09
defense response	9.82E-09
regulation of cellular process	2.31E-08
regulation of biological process	2.36E-08
biological regulation	3.48E-08
regulation of nitrogen compound metabolic process	5.94E-08
regulation of transcription	7.09E-08
response to abiotic stimulus	7.11E-08

Fig 6. ALE1, GSO1 and GSO2 positively regulate the expression of stress-related genes in seeds. (a) Summary of overlaps between gene sets showing reduced expression in *ale1-4* and *gso1-1 gso2-1* mutants at the globular and heart stages of development. (b) GO term analysis of genes down-regulated in both *ale1-4* and *gso1-1 gso2-2* mutants at the heart stage.

<https://doi.org/10.1371/journal.pgen.1007847.g006>

Expression of *ALE1* was not reduced in *gso1-1 gso2-1* mutants (S1 Table and S8 Fig), suggesting that *ALE1* is not a downstream target of GSO1 GSO2-mediated signalling, and could therefore act upstream of GSO1 and GSO2 in mediating embryonic responses necessary for the establishment of an intact embryonic cuticle.

MPK6 acts in the ALE1 GSO1 GSO2 signalling pathway

The GSO1 and GSO2 receptor kinases belong to family XI of the Leucine-Rich Repeat (LRR)-RLKs [34,35], and are closely related to the “danger” peptide receptors PEPR1 and PEPR2 [36,37], which are involved in the amplification of defence responses triggered by pathogen-associated molecular pattern (PAMP) perception [38]. A previous study [39], reported aberrantly shaped seeds, resembling those of *ale1-4* mutants, in Arabidopsis *mpk6* mutants lacking the MITOGEN ACTIVATED PROTEIN KINASE6 (MPK6) protein, which acts downstream of PEPR signalling. In addition a proportion of *mpk6* mutant seeds were reported to rupture [39]. We confirmed these phenotypes in the *mpk6-2* mutant background (S10 Fig). A recent article has suggested that some seed defects in *mpk6* mutants may depend upon the genotype of the maternal tissues in the seed [40]. Reciprocal crosses were therefore performed, and these confirmed that seed twisting phenotype is dependent upon the genotype of the zygotic compartment and not the maternal compartment (S11 Fig). Consistent with previous reports [39, 40] *mpk6-2* mutants produce embryos with highly variable phenotypes, around 30% of which fail to develop a normal hypocotyl region (“deformed” embryos Fig 7). We found that 40–50% of both deformed and normal *mpk6-2* embryos showed abnormal permeability to the hydrophilic dye toluidine blue, consistent with the presence of embryonic cuticle defects (Fig 7A). This phenotype correlated well with toluidine blue permeability phenotypes observed in etiolated seedlings, confirming that defects were not simply a consequence of abnormal development post-germination (Fig 7B). Auramine O staining of the cotyledons of etiolated seedlings was used to confirm *mpk6* cuticle defects (S12 Fig). Using this technique, wild-type cotyledons were found to be covered with a continuous cuticle layer. As previously reported, and consistent with our cutin analysis, *gpat4 gpat8* mutants showed drastically reduced cuticle staining. In contrast *gso1-1 gso2-1* mutants showed a patchy cuticle, similar to that seen using transmission electron microscopy on the embryo surface. Both *ale1-4* and *mpk6-2* mutants showed a more weakly stained cuticle than wild-type, which although apparently continuous, showed uneven cutin deposition (S12 Fig).

Triple *mpk6-2 gso1-1 gso2-1* and double *ale1-4 mpk6-2* mutants were generated to investigate further the genetic interactions of *ALE1*, *GSO1* and *GSO2* with *MPK6*. Fertility in *ale1-4 mpk6-2* double mutants was similar to that in *mpk6-2* mutants, while triple *mpk6-2 gso1-1 gso2-1* mutant plants were viable but produced very few seeds. In terms of seed shape and cotyledon cuticle permeability, triple *mpk6-2 gso1-1 gso2-1* mutants had phenotypes identical to those observed in *gso1-1 gso2-1* double mutants (Fig 7, S10 Fig). Since all *gso1-1 gso2-1* mutant seeds are twisted, non-additivity cannot be concluded from this phenotype. However, recent work has shown that additivity of toluidine blue staining phenotypes can be detected in mutant combinations with *gso1-1 gso2-1* [41]. The frequency of “twisted” seeds (including ruptured seeds), and toluidine blue stained seedling cotyledons was non-additive in *ale1-4 mpk6-2* double mutant plants, consistent with *ALE1*, *GSO1*, *GSO2* and *MPK6* acting in the same genetic pathway to control seedling cotyledon permeability (Fig 7 and S10 Fig).

MPK6 is involved in a plethora of reproductive and non-reproductive developmental processes and shows functional redundancy with other MPK proteins [39,42–52] meaning that global transcriptome analysis in the *mpk6-2* background would likely be uninformative for this study. We therefore directly tested a subset of genes mis-regulated in *gso1-1 gso2-1* and

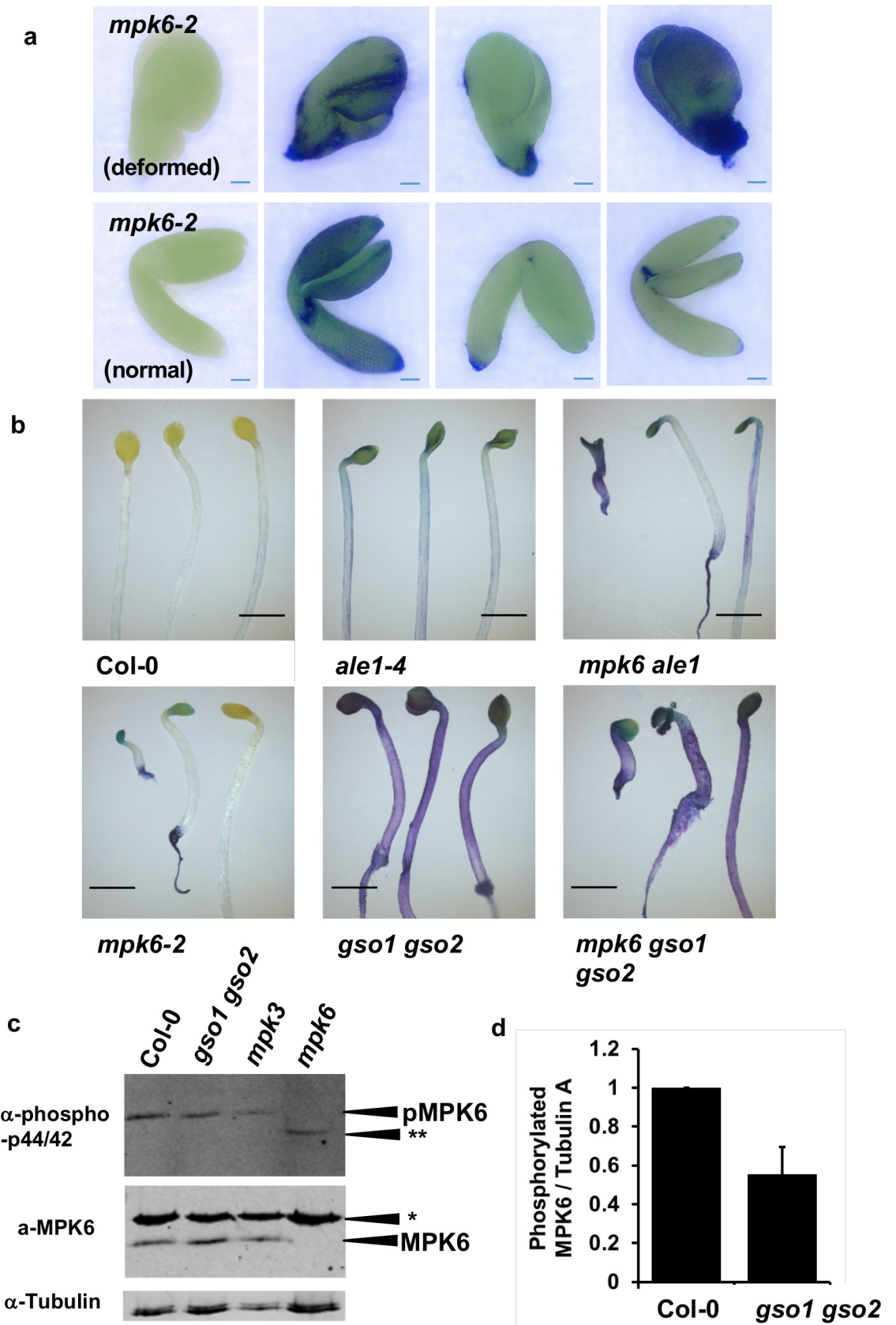


Fig 7. MPK6 acts downstream of ALE1, GSO1 and GSO2 mediated signalling. (a) Cuticle permeability phenotypes of fully expanded but immature *mpk6-2* embryos. Scale bar = 50 μ m. Representative unstained embryos are shown in the left-hand column, and a representative sample of stained embryos are shown in the following three columns (experiment carried out in parallel to that described in Fig 5). (b) Seedling cuticle permeability phenotypes of *mpk6-2* and *ale1-4* and *gso1-1 gso2-1* mutants and in double and triple mutant combinations. Scale bar = 2mm (c) Analysis of proteins extracted from developing seeds at the globular-early torpedo stage. The mutants *mpk3-1* and *mpk6-2* were included to confirm band identification. No phosphorylation of MPKs other than MPK6 is observed in Col-0, *gso1-1 gso2-1* or *mpk3-1* seeds, but an additional band (***) is systematically observed in the *mpk6-2* mutant background. * Indicates a non specific band detected by the anti-MPK6 antibody. This experiment was repeated 7 times on independent biological samples, with similar results. (d) Degree of phosphorylation of MPK6 in Col-0 and *gso1-1 gso2-1* mutant seeds. Error bars represent SD of 3 biological replicates (see S16 Fig for linearity testing).

<https://doi.org/10.1371/journal.pgen.1007847.g007>

ale1-4 mutants for misregulation in *mpk6-2* mutants at three stages of embryo development. Five out of eight genes tested showed reduced expression in *mpk6-2* either at all three stages (*SWI3A*, *WRKY70* and *NIMIN1*), or in two out of three developmental stages tested (*SIB1* and *NIMIN2*) (S13 Fig). Unsurprisingly given the relatively weak cuticle phenotype of *mpk6* mutants compared with *gso1 gso2* mutants, some genes showing strong down-regulation in the *gso1-1 gso2-1* mutants (*WRKY33*, *WRKY46* and *WRKY53*) did not show any significant reduction in expression in the *mpk6-2* mutant background (S13 Fig) indicating that their transcriptional regulation downstream of GSO1 and GSO2-mediated signalling could be dependent on signalling components acting redundantly with MPK6. The expression of *ALE1*, *GSO1* and *GSO2* was not altered in *mpk6-2* mutants (S13 Fig), indicating that MPK6 most probably acts downstream of GSO1 and GSO2-mediated signalling.

To further confirm this hypothesis, we analysed MPK phosphorylation in developing seeds from Col-0 and *gso1-1 gso2-1* double mutants. In seedlings, phosphorylation of MPK6 (and additional MPKs) can only be detected after elicitation (for example with the flg22 peptide). The response to flg22 is not attenuated in *gso1/gso2* mutant seedlings (S14 Fig and S15 Fig). In contrast, MPK6 phosphorylation (but not phosphorylation of other MPKs) could be detected in un-elicited seeds (Fig 7C and S16 Fig). Following quantification, we found that the degree of phosphorylation of MPK6 was reduced by approximately 50% in *gso1-1 gso2-1* double mutant seeds compared to wild-type, suggesting that a significant proportion of MPK6 phosphorylation in seeds depends on the activity of GSO1 and GSO2 (Fig 7D, S16 Fig). Intriguingly, in seeds, a band corresponding to a second phosphorylated MPK was detected exclusively in *mpk6-2* mutants (Fig 7C), suggesting that the relatively weak *mpk6* seedling cuticle phenotype could be due to compensation by an as yet unidentified MPK [53].

MPK6 activity is required in the embryo, but not the endosperm, to maintain cuticle integrity

The strong expression of GSO1 and GSO2 in the embryonic epidermis, suggests that the activity of GSO1 and GSO2 in cuticle formation is required in the embryo. No promoters confirmed as specifically being expressed only in the embryo or embryo epidermis, have been published. To further confirm the spatial requirement for GSO1/GSO2-dependent signalling in the seed, we therefore complemented the *mpk6-2* mutant either with the *MPK6* cDNA expressed under the ubiquitously expressed *RPS5A* promoter, or under the endosperm specific *RGP3* promoter [54,55]. We were unable to complement either the misshapen seed/seed bursting phenotypes or the toluidine blue permeability phenotypes of *mpk6-2* mutants by expressing *MPK6* in the endosperm, but obtained full complementation of all phenotypes in plants expressing *MPK6* under the *RPS5A* promoter (Fig 8, S17 Fig). Together with the results of our reciprocal crosses, these findings indicate that the seedling permeability phenotype of *mpk6-2* mutants is most likely due to signalling defects in the embryo. Seed size and seed bursting defects could be caused by lack of MPK6 in the testa, as suggested by reciprocal crosses,

although this remains to be investigated in more detail. In order to further confirm the function of MPK6 downstream of GSO1/GSO2 signalling we attempted to express a constitutively active form of MPK6 under the *RPS5A* promoter in wild type and double mutant plants, but were unable to generate any transformants, potentially due to the critical roles played by MPK6 during early embryogenesis.

Discussion

In this study, consistent with the similarity between GSO1/2 and PEPR1/2 proteins, we found that stress-associated kinase MPK6, which has been shown to act downstream of PEPR signalling [56], shows constitutive phosphorylation in developing seeds, and that this phosphorylation is partially dependent upon GSO1 and GSO2. In addition, we showed that GSO1/GSO2 are required for the expression of a set of stress-related genes during early seed development. Our results suggest that GSO1/GSO2 dependent stress response-related signalling pathways are active in developing seeds. Because of the conserved transcriptional targets expressed downstream of GSO1/GSO2 dependent signalling, and in defence responses, this scenario is distinct from previously reported situations in which single pathway components, such as the co-receptor BAK1, play distinct roles in developmental and defence-related signalling cascades through interaction with multiple receptors [57,58]. However, the role of the transcriptional targets of GSO1/GSO2 signalling in seeds remains to be elucidated.

Our work also shows that GSO1/GSO2, ALE1 and MPK6 act in a genetic pathway involved in ensuring embryonic cuticle integrity. We show for the first time that embryonic cuticle biogenesis involves the coalescence of discontinuous patches of cutin-like material that appear on the embryo surface at the globular stage, and that pathway mutants are either incapable of completing, or retarded in the completion of “gap closure” during this process. Interestingly, GSO1 (also known as SCHENGEN3 [6]) was recently shown to be involved in ensuring the continuity of another apoplastic diffusion barrier, the Casparian strip, which prevents the apoplastic movement of solutes from the cortex to the stele of the root [6]. GSO1 may therefore form part of a general mechanism employed by plants for monitoring the “integrity” of apoplastic barriers formed during plant development.

The role of GSO1 and GSO2 in the closure of gaps in the nascent cuticle implies spatial regulation of signalling outputs at the subcellular level. Cytoplasmic signalling components which, like MPK6 might not be uncovered by transcriptome analysis but instead be modified post-translationally, are therefore likely to be of critical importance in GSO1 GSO2 signalling in the embryonic epidermis. Indeed, although MPK6-mediated signalling has most often been implicated in the control of transcription, particularly via the modulation of the activity of WRKY transcription factors, evidence for potential roles in cytoplasmic responses, for example during funicular guidance of pollen tubes [46] and control of cell division planes [50], exist in the literature.

Cytoplasmic responses downstream of receptor-like kinases include the local production of apoplastic Reactive Oxygen Species (ROS) and/or calcium influxes, and indeed localized ROS production has been implicated in Casparian strip formation [6,59–61]. However although a plausible model has proposed that ROS release could mediate Casparian strip polymerisation through polymerisation of monolignols [59], it is less obvious how ROS could directly affect the biosynthesis of an aliphatic cutin-based barrier, although a possible role for ROS in linking the cuticle to the cell wall has been evoked [62]. ROS production has been shown to directly modulate the activation of MAPK signalling, providing a mechanism permitting the reinforcement of localised signalling events [63,64]. Another, potentially linked, possibility is that GSO1/GSO2 activity in the embryo could spatially direct the secretion of either cuticle components

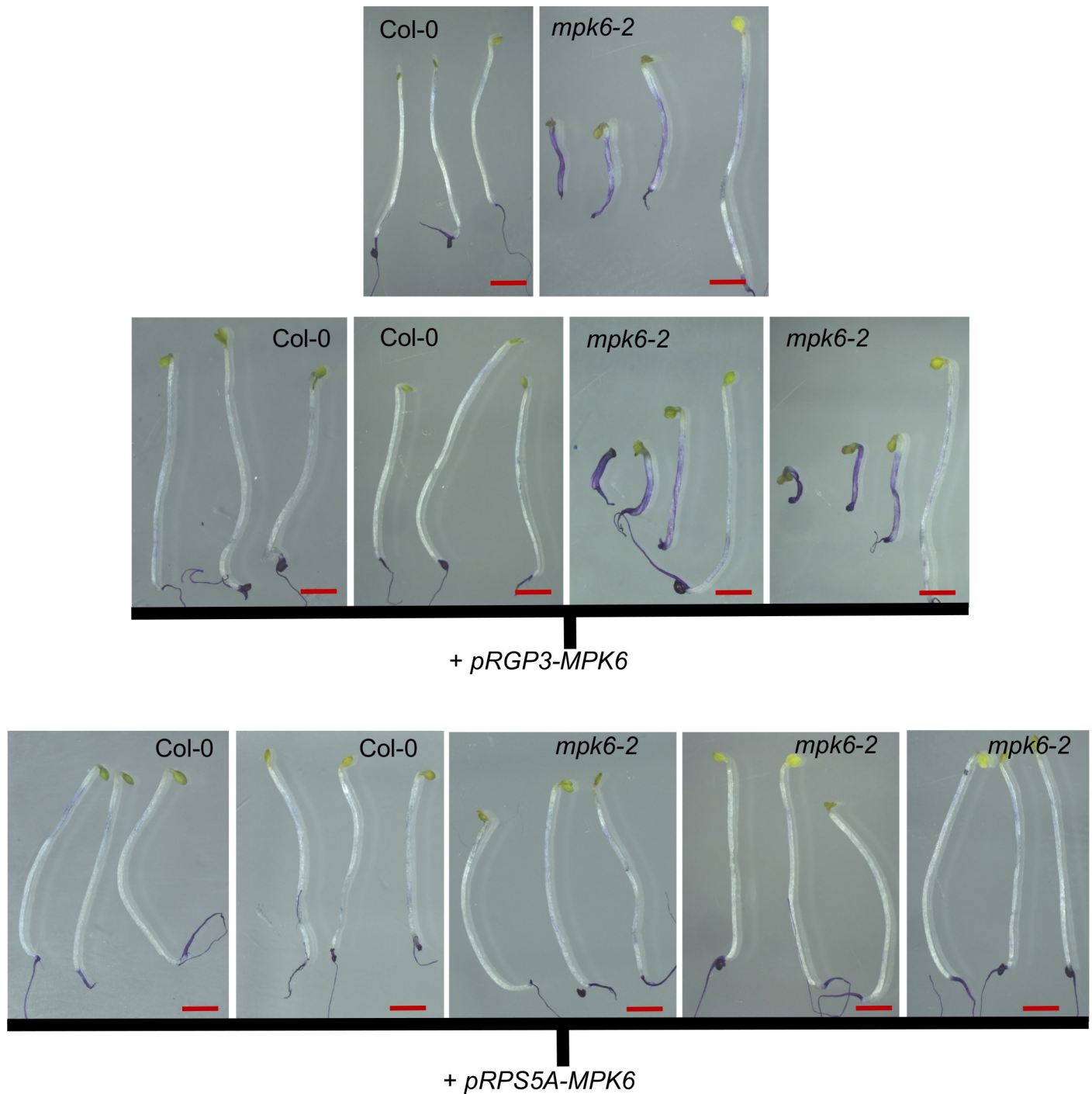


Fig 8. MPK6 activity is required in the embryo and testa, but not the endosperm, for normal seedling development. Representative phenotypes of toluidine blue-stained seedlings from wild-type (Col-0), *mpk6-2*, and these backgrounds transformed with *pRGP3-MPK6* or *pRPS5A-MPK6*. Lines correspond to those described in S17 Fig. Scale bar = 2mm.

<https://doi.org/10.1371/journal.pgen.1007847.g008>

or enzymes and cell wall components necessary for their integration into the cutin polymer, in a system analogous to the rapid and highly localized deposition of callose observed upon hyphal penetration into epidermal cells (reviewed in [65,66]). Interestingly MPK6 has also

been shown to be involved in phragmoplast formation during root cell division and therefore could be involved in the localised production/secretion of apoplastic compounds [50]. However, observing these processes *in situ*, within the living seeds, would require developments in microscopy which are not yet available.

Our work highlights several questions which merit further discussion. A first important question is whether the GSO1/GSO2 signalling pathway could play a role in protecting seeds, or more generally plants, against pathogen attack. Cuticle integrity in adult plants has been shown to be required for resistance to *Pseudomonas* pathogens [67,68]. The action of the ALE1 GSO1/GSO2 signalling pathway in ensuring embryonic cuticle integrity is therefore likely to have a significant influence on embryo and seedling susceptibility to bacterial pathogens. However, we have also shown that GSO1/GSO2, ALE1 and MPK6 are necessary for the expression of known defence marker genes in seeds. Cuticle permeability phenotypes have not been reported in the literature for mutants affected in the defence markers identified in our transcriptome studies. This raises the question of whether the ALE1, GSO1/GSO2, MPK6 signalling pathway, in addition to mediating localised apoplastic modifications, could act at a more global level either to protect developing seeds from the ingress of bacterial pathogens (thus affecting vertical pathogen transmission), or to “prime” embryos against pathogen attack upon germination. Exploring this possibility would necessitate functionally separating susceptibility caused by cuticle defects from lack of immune priming, and will be technically very challenging, but could ultimately inform strategies aiming to reduce vertical transmission of plant pathogens.

The second question concerns how signalling via GSO1 and GSO2 is triggered in the seed in the absence of pathogens. In this study we consolidate data supporting the function of ALE1 in the same pathway as GSO1 and GSO2. We previously proposed that the function of ALE1, GSO1 and GSO2 in ensuring the apoplastic separation of the embryo and endosperm became necessary in angiosperms due to developmental constraints imposed by the sexualisation of the female gametophyte, which led to the simultaneous development of the embryo and surrounding nutritive tissues post-fertilization, rather than their sequential development [11,12]. ALE1 expression is endosperm specific and, as previously suggested [69], the recruitment of ALE1 to a function in reinforcing the embryonic cuticle may have occurred during the emergence of the angiosperm lineage. The fact that the phenotype of *ale1* mutants is weaker than that of *gso1 gso2* double mutants, particularly at later stages of embryogenesis, may be due to redundancy with other members of the subtilase family in Arabidopsis, several of which are encoded by genes expressed in the developing endosperm [19,20]. Subtilases have been shown to be involved in defence responses and immune priming in plants [70,71]. It is thus possible that ALE1 acts to produce an as yet unidentified ligand for the GSO1 and GSO2 receptors. In such a scenario the function of ALE1 in the seed could be analogous to the “immune priming” function previously reported for the subtilase SBT3.3 [71].

Such a scenario naturally raises a third, and important question, around the identity of the ligand of GSO1 and GSO2. Two sulfated peptides, CIF1 and CIF2, which can act as ligands for GSO1 during Casparian strip formation, have recently been identified [72,73]. Testing the role of these molecules in developing seeds will be an obvious priority. However Nakayama and colleagues specifically reported that no cuticle defects (as gauged by cotyledon fusion phenotypes) were observed in *cif1 cif2* double mutants and the possibility that other signalling molecules could be involved in ensuring embryonic cuticle integrity therefore cannot be excluded.

In summary, we propose that endosperm-localised factors (like ALE1) may have been recruited to hijack a defence-signalling pathway involving the ancestor(s) of GSO1 and GSO2, and downstream signalling components including MPK6, and trigger an “auto-immune” type response in the embryo to ensure cuticle integrity. The future identification of further pathway

components, and in particular the substrates of ALE1 and ligands of GSO1 and GSO2, will help to confirm this hypothesis.

Materials and methods

Plant material

The *pGSO1:GSO1-mVENUS* line was kindly donated by Professor Niko Geldner (Unil-Sorge, University of Lausanne). The *mpk6-2* (SALK_073907) mutant and the *mpk3-1* (SALK-151594) were kindly provided by Dr Roberta Galletti.

Growth conditions and plant treatments

Unless otherwise specified, plants were grown for 10 d in sterile conditions on Murashige and Skoog (MS) agar plates with 0.5% sucrose, 1 month under short-day conditions (19°C, 8h light / 17°C, 16h dark) and then transferred to standard long-day conditions (21°C, 16h light/ 8h dark) for one more month. To stage material, newly opened flowers were marked each day for two weeks. For bacterial growth assays, plants were grown under controlled conditions in a growth chamber at 21°C, with a 9-hours light period and a light intensity of 190 $\mu\text{mol}\cdot\text{m}^{-2}\cdot\text{s}^{-1}$. For MPK6 activation analysis, seedlings were grown for 10 d in MS liquid medium supplemented with 0.5% sucrose in 100 μm cell strainers submerged in 6-well plates (5ml of medium per well). Cell strainers were transferred to new plates containing MS sucrose 0.5% supplemented with 100 nM or 1 nM flg22 or water and incubated for 15 and 60 minutes at room temperature without shaking. Seedlings were then rapidly harvested in liquid nitrogen and stored at -80°C until protein extraction. For cutin analysis of seedlings, seeds were sterilized, plated on MS medium supplemented with 0.7% agar, 0.7% sucrose and 2.5 mM MES-KOH, pH 5.7, and stratified in the dark for 3 days at 4°C. Plates were then transferred to a controlled environment growth chamber at 22°C and with continuous light, and seedlings were grown for 5 days before harvesting the cotyledons. For toluidine blue staining and Auramine O staining, sterilized seeds were spread uniformly on 15 cm MS plates with 0.5% sucrose and 0.4% Phytigel (Sigma) (pH 5.8) and stratified for 2 days in the dark at 4°C. After stratification seeds were transferred to a growth chamber and incubated for 6h under continuous light followed by 4 days in the dark.

In situ hybridization

DNA templates for the probes used in *in situ* hybridizations were amplified using the primers listed in [S2 Table](#). Digoxigenin-labelled RNA probes were produced and hybridized to tissue sections following standard procedures. In brief, siliques were opened, fixed overnight in ice-cold PBS containing 4% paraformaldehyde, dehydrated through an ethanol series, embedded in Paraplast Plus (Mc Cormick Scientific) and sectioned (8 μm). Immobilized sections were dewaxed and hydrated, treated with 2x saline sodium citrate (20 min), digested for 15 min at 37°C with proteinase K (20 mg/ml) in 50mM Tris-HCl, pH 7.5, 5mM EDTA), treated for 2 min with 0.2% glycine in PBS, rinsed, post-fixed with 4% paraformaldehyde in PBS (10 min, 4°C), rinsed, treated with 0.25% w/v acetic anhydride in 100mM triethanolamine (pH 8.0 with HCl) for 10 min, rinsed and dehydrated. Sections were then hybridized under coverslips overnight at 50°C with RNA probes (produced using DIG RNA labelling kit (Roche)) diluted in DIG easy Hyb solution (Roche) following the manufacturer's instructions. Following hybridization, the slides were extensively washed in 0.1x saline sodium citrate and 0.5% SDS at 50°C (3 h), blocked for 1 hour in 1% blocking solution (Roche) in TBS and for 30 minutes in BSA solution (1% BSA, 0.3% Triton-X-100, 100mM Tris-HCl, 100mM NaCl, 50mM MgCl_2), and

then incubated in a 1/3000 dilution of in alkaline phosphatase-conjugated antidigoxigenin antibody (Roche) in BSA solution for 2h at RT. Sections were extensively washed in BSA solution, rinsed and treated overnight in the dark with a buffered NBT/BCIP solution. Samples were rinsed in water before air drying and mounting in Entellan (Sigma).

Microscopy

Embryos were imaged by gently bursting seeds between slide and cover-slip in water and imaging using a dipping lens with a long working distance. Confocal imaging was carried out on a Zeiss LSM700 with a W N-Acroplan 40x/0.75 M27 objective. mVENUS was excited using a 488nm diode laser and fluorescence was collected using a 490–555 nm PMT. Light microscopy imaging was carried out using a Zeiss axioimager 2. Images were acquired using bright field illumination.

Histochemical staining with Auramine O

4-day-old etiolated seedlings were fixed with 4% PFA (paraformaldehyde) (Sigma-Aldrich) in 1X PBS with at least 1 hour under vacuum as described in [74]. Fixed seedlings were washed twice for 1 min in 1X PBS before being transferred for at least 6-days to ClearSee solution (10% w/v xylitol (Sigma-Aldrich); 15% w/v sodium deoxycholate (Sigma-Aldrich); 25% w/v urea (Sigma-Aldrich); water) at room temperature with gentle agitation. Cleared etiolated seedlings were stained with a 0.5% solution of Auramine O (Sigma-Aldrich) in ClearSee. After 12–16 hours of incubation in the dark, seedlings were washed briefly in ClearSee then washed again for 30min and then again for at least 1h before being placed between slide and coverslip with ClearSee as the mounting solution. Confocal imaging was performed using a Zeiss LSM700 with a Plan-Apochromat 63x/1.4 oil DIC M27 (ref 420782–9900) objective. Auramine O fluorescence was imaged with a 488nm diode laser excitation and detection of emission from 505–530nm. Images were then processed in the Zeiss LSM Image Browser Program.

Cutin analysis

Cuticle composition and content was analyzed as previously described [75,76].

TEM analysis

For transmission electron microscopy analysis, seeds were removed from siliques by removal of the replum tissue with attached seeds. Seeds were high-pressure frozen with a Leica EM-PACT-1 system. Three seeds were inserted into a flat copper carrier, fast-frozen, and cryo-substituted into the Leica AFS1 device. The different freeze-substitution steps were as follows: 54 h at -90°C in acetone solution containing 0.2% glutaraldehyde, 1% osmium tetroxide, and 0.1% uranyl acetate. The temperature was then raised with a step of $2^{\circ}\text{C}/\text{h}$ before remaining for 8 hours at -60°C . The temperature was raised again to -30°C for 8h00 before being increased to 4°C . Samples were washed three times for 10 min in 100% acetone before embedding in Spurr's resin, which was performed progressively (8 h in 25% Spurr's resin in acetone, 24 h in 50% Spurr's resin in acetone, 24 h in 75% Spurr's resin in acetone, and two times for 12 h in 100% Spurr's resin). Polymerization was performed at 70°C for 18 h.

Samples were sectioned (65 nm sections) and imaged at 120 kV using an FEI TEM tecnai Spirit with 4 k x 4 k eagle ccd.

Generation of micro-array data

Microarray analysis was carried out at a Transcriptomic Platform, POPS, at the Institute of Plant Sciences Paris-Saclay (IPS2, Orsay, France), using a CATMAv7 array based on AGILENT technology [77]. The CATMAv7 array for the Arabidopsis thaliana genome was made using gene annotations included in FLAGdb++, an integrative database of plant genomes (<http://urgv.evry.inra.fr/FLAGdb>, [78]). The single high density CATMAv7 microarray slide contains four chambers, each containing 149 916 primers. Each 60 bp primer is present in triplicate in each chamber for robust analysis, and as both strands. The array contains 35 754 probes (in triplicate) corresponding to genes annotated in TAIRv8 (among which 476 probes correspond to mitochondrial and chloroplast genes), 1289 probes corresponding to EUGENE software predictions, 658 probes to miRNA/MIRs and 240 control probes.

3 independent biological replicates were produced. For each biological repetition and each point, RNA samples were obtained by pooling RNAs from staged siliques containing embryos at the pre-globular to globular, or the young to late heart stage. Total RNA was extracted using the Spectrum Plant Total RNA Kit (Sigma-Aldrich) according to the suppliers' instructions. For each comparison, one technical replicate with fluorochrome reversal was performed for each biological replicate (i.e. four hybridizations per comparison). The labelling of cRNAs with Cy3-dUTP or Cy5-dUTP was performed as described in the Two-Color Microarray-Based Gene Expression Analysis Low Input Quick Amp Labelling manual (Agilent Technologies, Inc.). The hybridization and washing steps were performed according to the Agilent Microarray Hybridization Chamber User Guide instructions ((Agilent Technologies, Inc.). Two micron scanning was performed with InnoScan900 scanner (Innopsys, Carbonne, FRANCE) and raw data were extracted using Mapix software (Innopsys, Carbonne, FRANCE).

Statistical analysis of microarray data

Experiments were designed with the statistics group of the Unité de Recherche en Génomique Végétale. For each array, the raw data comprised the logarithm of median feature pixel intensity at wavelengths 635 nm (red) and 532 nm (green). For each array, a global intensity-dependent normalization using the loess procedure [79] was performed to correct the dye bias. The differential analysis was based on log-ratio averaging over the duplicate probes and over the technical replicates. Hence the number of available data points for each gene equals the number of biological replicates and is used to calculate the moderated t-test [80]. Analysis was carried out using the R software (<http://www.R-project.org>). Under the null hypothesis, no evidence that the specific variances vary between probes was highlighted by Limma and consequently the moderated t-statistic was assumed to follow a standard normal distribution. To control the false discovery rate, adjusted p-values found using the optimized FDR approach [81] were calculated. We considered as being differentially expressed, the probes with an adjusted p-value ≤ 0.05 . The function SqueezeVar of the library Limma was used to smooth the specific variances by computing empirical Bayes posterior means. The library kerfdr was used to calculate the adjusted p-values.

Data deposition

Microarray data from this article were deposited at Gene Expression Omnibus (<http://www.ncbi.nlm.nih.gov/geo/>), accession no. GSE68048) and at CATdb (http://tools.ips2.u-psud.fr/cgi-bin/projects/CATdb/consult_project.pl?project_id=383) according to the "Minimum Information About a Microarray Experiment" standards.

Quantitative gene expression analysis in seeds

Intact siliques were frozen in liquid nitrogen and total RNA was extracted using the Spectrum Plant Total RNA Kit (Sigma). Total RNAs were digested with Turbo DNA-free DNase I (Ambion) according to the manufacturer's instructions. RNA was reverse transcribed using the SuperScript VILO cDNA Synthesis Kit (Invitrogen) according to the manufacturer's protocol. PCR reactions were performed in an optical 384-well plate in the QuantStudio 6 Flex System (Applied Biosystems), using FastStart Universal SYBR Green Master (Rox) (Roche), in a final volume of 10 μ l, according to the manufacturer's instructions. The following standard thermal profile was used for all PCR reactions: 95°C for 10 min, 40 cycles of 95°C for 10 s, and 60°C for 30 s. Data were analysed using the QuantStudio 6 Flex Real-Time PCR System Software (Applied Biosystems). As a reference, primers for the EIF4A cDNA were used. PCR efficiency (E) was estimated from the data obtained from standard curve amplification using the equation $E = 10^{-1/\text{slope}}$. Expression levels are presented as $E^{-\Delta C_t}$, where $\Delta C_t = C_{t_{GOI}} - C_{t_{EIF4A}}$. Primers are listed in [S2 Table](#).

Toluidine blue staining

The lids of plates containing etiolated seedlings were removed and plates were immediately flooded with staining solution [0.05% (w/v) Toluidine Blue + 0.4% (v/v) Tween-20] for one minute. The staining solution was poured off and plates were immediately rinsed gently by flooding under a running tap until the water stream was no longer visibly blue (1–2 minutes). Seedlings were photographed under a Leica MZ12 stereomicroscope. For embryo staining, flowers were marked at anthesis and seeds were dissected from siliques of the same age for all genotypes in parallel. Embryos were removed from seeds by dissection with fine forceps and placed in handling baskets, which were then submerged in toluidine blue solution for one minute prior to rinsing 5 times in an excess of tap water. Embryos were photographed using a Keyence VHX-900 microscope.

Protein extraction and MPK6 activation analysis

Seedlings or seeds were quickly frozen in liquid nitrogen and proteins were extracted in buffer containing 50 mM Tris pH 7.5, 200 mM NaCl, 1 mM EDTA pH 8, 10% glycerol, 0.1% tween 20, 1 mM phenylmethylsulfonyl fluoride, 1 mM dithiothreitol, 1x protease inhibitor cocktail P9599 (Sigma-Aldrich), and 1x MS-Safe protease and phosphatase inhibitor cocktail (Sigma-Aldrich). Equal amounts of proteins (20 μ g for seedlings and 10 μ g for seeds) were resolved on 10% polyacrylamide gels and transferred onto a nylon membrane (Schleicher & Schuell). For seedlings primary antibodies against phospho p44/42 MAP kinase (1:2000 dilution) (Cell Signaling Technologies) and then against MPK6 (1:10000 dilution) (Sigma-Aldrich) were used with horseradish peroxidase-conjugated anti-rabbit as secondary antibody. Signal detection was performed using the SuperSignal West Femto Maximum Sensitivity Substrate kit (Pierce). For seeds primary antibodies against phospho p44/42 MAP kinase and then against MPK6 were used with IRDye 800CW Donkey anti-Rabbit IgG (H + LI-COR, 1:10000 dilution), and the bound complex was detected using the Odyssey Infrared Imaging System (Li-Cor; Lincoln, NE). The images were analysed and quantified with ImageJ. Background was subtracted for each band. To test the linearity of the detection, 5–15 μ g protein from heart stage developing seeds were treated as previously. To detect the antibody against phospho p44/42 MAP kinase an anti-Rabbit IgG, HRP conjugate (Amersham, 1:30000) was used. Anti-alpha-tubulin (Sigma, 1:2000) was used with an anti-mouse IgG, HRP conjugate (GE HealthCare, 1:10000). Signal detection was performed using Clarity Max Western ECL Substrate (Biorad) with a

ChemiDoc Touch (Biorad) instrument. The images were quantified with ImageJ. Background was subtracted for each band.

Supporting information

S1 Fig. (Related to Fig 1): Genes involved in cuticle biosynthesis are expressed early during embryo development and are co-expressed with GSO1 and GSO2. Expression data for *LACS2* (a), *FDH* (b), *BDG* (c), *LCR* (d), *LTPG1* (e), *ABCG11* (f), *GSO1* (g) and *GSO2* (h) downloaded from the Seed Gene Network resource (<http://seedgenenetwork.net/>). (TIF)

S2 Fig. (Related to Fig 1): Genes involved in cuticle biosynthesis are co-expressed with GSO1 and GSO2 in the embryonic epidermis during embryogenesis, but their expression is not dependent upon GSO1 and GSO2. Analysis of the expression of genes involved in cuticle biosynthesis in wild-type (Col-0) and *gso1-1 gso2-1* seeds containing late globular/triangle, heart and early torpedo stage embryos (left to right). (TIF)

S3 Fig. (Related to Fig 1): Hybridization of tissue sections to an antisense GFP probe as negative control in Col-0 (a-c) and *gso1 gso2* (d-f) seeds containing late globular (a,d), heart (b,e) and early torpedo (c,f) stage embryos. Expression of *LTPG1* in wild type seed containing torpedo stage embryo is shown in (g) for direct comparison. (TIF)

S4 Fig. (Related to Fig 4): Cuticle discontinuities in early wild-type (Col-0) embryos and later *gso1 gso2* embryos. a,b) Cuticle the mid-late globular stage (during gap closure) in Col-0 embryos showing discontinuous cuticle. *gso1-1 gso2-1* mutant embryos maintain a diffuse and discontinuous cuticle at later stages. Analysis of embryonic cuticle deposition in *gso1-1 gso2-1* at the *mid heart* (c-d) and walking stick (e-f) stages of embryogenesis, when wild-type cuticle is continuous. White arrows show external face of embryonic cuticle. Scale bar = 500nm. (TIF)

S5 Fig. (Related to Fig 4): Analysis of the permeability of extruded Col-0 embryos at different developmental stages to toluidine blue treatment. Three stained and one unstained embryo (lower tier) are shown for each developmental stage. Stages are a) late heart-early torpedo, b) mid torpedo, c) late torpedo, d) walking stick-bent cotyledon, e) late bent cotyledon, f) fully expanded immature. Scale bar = 100µm. (TIF)

S6 Fig. (Related to Fig 6): GO term analysis of genes showing increased expression in siliques of both *gso1-1 gso2-1* and *ale1-4* mutant backgrounds at the globular (a) and heart (b) stages of embryo development. The degree of overlap between these datasets is illustrated in (c). (TIF)

S7 Fig. (Related to Fig 6): GO term analysis of genes showing reduced expression in siliques of both *gso1-1 gso2-1* and *ale1-4* mutant backgrounds at the globular (a) and heart (b) stages of embryo development. (TIF)

S8 Fig. (Related to Fig 6): Validation by qRT-PCR of microarray data. Experiments were carried out in 4 biological replicates. Values are expressed relative to the *EIF4A* gene. Significance values indicated were calculated using a Student's t-test. *** denotes $p < 0.01$, ** denotes

$p < 0.05$ and * denotes $p < 0.1$. Bars indicate standard errors.
(TIF)

S9 Fig. (Related to Fig 6): Analysis of the expression of *SWI3A* in wild-type (a-c), *gso1-1 gso2-1* (d-f) mutant embryos in seeds containing late globular/triangle (a,d), heart (b,e) and early torpedo (c,f) stage embryos. Expression data for *SWI3A* downloaded from the Seed Gene Network resource (<http://seedgenenetwork.net/>) is shown in (g).
(TIF)

S10 Fig. (Related to Fig 7): Non additivity of seed twisting (a-b) and seedling cuticle permeability (c) phenotypes between *mpk6-2* and *ale1-4* mutants and between *mpk6-2* and *gso1-1 gso2-1* double mutants. Populations of seeds (a) from single double and triple mutants were photographed, and seed phenotypes were quantified (b) (Col-0 $n = 196$, *ale1-4* $n = 200$, *mpk6-2* $n = 210$, *gso1-1 gso2-1* $n = 111$, *mpk6-2 ale1-4* (3 individuals) $n = 211, 212$ and 238 , *mpk6-2 gso1-1 gso2-1* $n = 86$). Etiolated seedlings were treated with toluidine blue and seedling and toluidine blue phenotypes were quantified (c). Results are representative of three independent experiments. Col-0 $n = 389$, *ale1-4* $n = 387$, *mpk6-2* $n = 383$, *mpk6-2 ale1-4* $n = 398$. (Quantifications were not possible for *mpk6-2 gso1-1 gso2-1* triple mutants due to low seed set).
(TIF)

S11 Fig. (Related to Fig 7): Seed twisting phenotypes of *mpk6* mutants are dependent upon the zygotic genotype. Phenotypes of seeds resulting from reciprocal crosses between *mpk6-2* mutant and wild-type plants. Twisted seeds were found in significant numbers only in self-pollinated siliques. This result was obtained for 2 independent crosses.
(TIF)

S12 Fig. (Related to Fig 7): Cuticle phenotypes using Auramine O staining of etiolated cotyledons. Genotypes are indicated on left panels with zones magnified on the right highlighted by white boxes. Arrows indicate position of the cuticle (dark line) and arrowheads indicate gaps in the cuticle.
(TIF)

S13 Fig. (Related to Fig 7): qRT-PCR analysis of the expression of candidate target genes in *mpk6-2* mutant siliques. Experiments were carried out in biological triplicate. Values are expressed relative to *EIF4* gene expression. Significance values indicated were calculated using a Student's t-test. *** denotes $p < 0.01$, ** denotes $p < 0.05$ and * denotes $p < 0.1$. Bars indicate standard errors.
(TIF)

S14 Fig. (Related to Fig 7): GSO1 and GSO2 are not necessary for MPK6 phosphorylation in response to PAMP-elicitation in seedlings. Western blot analysis of phosphorylated MPK proteins (upper panel) and then total MPK6 protein (middle panel). Loading control (Ponceau S-stained Rubisco) is shown in lower panel. The same blot is shown in the upper middle and lower panel. * Indicates a non specific band detected by the anti-MPK6 antibody. Seedlings were treated with water or with 100nM flg22 for either 15 or 60 minutes before protein extraction. The mutants *mpk3-1* and *mpk6-2* were included to confirm band identities.
(TIF)

S15 Fig. (Related to Fig 7): *gso1 gso2* mutant seedlings are not significantly affected in the MPK6 phosphorylation response to flg22. Western blot analysis of phosphorylated MPK proteins (upper panels) and then total MPK6 protein (middle panels). Loading control

(Ponceau S-stained Rubisco) is shown in lower panel. The same blot is shown in the upper middle and lower panel. * Indicates a non specific band detected by the anti-MPK6 antibody. Seedlings were treated with water or with 1nM flg22 for either 15 or 60 minutes before protein extraction.

(TIF)

S16 Fig. (Related to Fig 7): Developing *gso1 gso2* mutant seeds show reduced levels of MPK6 phosphorylation compared to wild-type seeds. a) Western blot analysis of phosphorylated MPK6 protein in developing seeds exposed at four consecutive one minute intervals (to confirm signal linearity). Loading control (α -tubulinA) is shown in lower panel. B) Degree of phosphorylation of MPK6 in Col-0 and *gso1-1 gso2-1* mutant seeds. Error bars represent SD of 3 biological replicates.

(TIF)

S17 Fig. (Related to Fig 8): MPK6 is required in the embryo and testa, but not the endosperm. (a) Representative phenotypes of seeds from wild-type (Col-0), *mpk6-2*, and these backgrounds transformed with *pRGP3-MPK6* or *pRPS5A-MPK6*. (b) Quantification of seed phenotypes in the above material. Seeds from at least two independent transgenic lines have been quantified.

(TIF)

S1 Table. Misregulated gene lists.

(XLSX)

S2 Table. Primers used in this study.

(TIFF)

Acknowledgments

We would like to thank Professor N. Geldner for providing seeds, and A. Lacroix, J. Berger, P. Bolland, H. Leyral and I. Desbouchages for assistance with plant growth and logistics.

Author Contributions

Conceptualization: Frédéric Domergue, Gwyneth Ingram.

Data curation: Audrey Creff, Lysiane Brocard, Ludivine Taconnat.

Formal analysis: Jérôme Joubès, Ludivine Taconnat, Nicolas M. Doll, Stéphanie Pascal, Frédéric Domergue.

Funding acquisition: Frédéric Domergue, Gwyneth Ingram.

Investigation: Audrey Creff, Lysiane Brocard, Nicolas M. Doll, Steven Moussu, Gwyneth Ingram.

Methodology: Audrey Creff, Lysiane Brocard, Nicolas M. Doll, Anne-Charlotte Marsollier, Stéphanie Pascal, Roberta Galletti, Sophy Boeuf, Frédéric Domergue, Gwyneth Ingram.

Project administration: Frédéric Domergue, Gwyneth Ingram.

Resources: Roberta Galletti.

Supervision: Jérôme Joubès, Thomas Widiez, Frédéric Domergue, Gwyneth Ingram.

Validation: Audrey Creff, Anne-Charlotte Marsollier.

Visualization: Audrey Creff, Lysiane Brocard, Anne-Charlotte Marsollier.

Writing – original draft: Audrey Creff, Jérôme Joubès, Ludivine Tacconnat, Roberta Galletti, Steven Moussu, Frédéric Domergue, Gwyneth Ingram.

Writing – review & editing: Audrey Creff, Thomas Widiez, Frédéric Domergue, Gwyneth Ingram.

References

- Ingram GC (2010) Family life at close quarters: communication and constraint in angiosperm seed development. *Protoplasma* 247: 195–214. <https://doi.org/10.1007/s00709-010-0184-y> PMID: 20661606
- Baroux C, Spillane C, Grossniklaus U (2002) Evolutionary origins of the endosperm in flowering plants. *Genome Biol* 3: reviews1026.
- Fiume E, Fletcher JC (2012) Regulation of Arabidopsis embryo and endosperm development by the polypeptide signaling molecule CLE8. *Plant Cell* 24: 1000–1012. <https://doi.org/10.1105/tpc.111.094839> PMID: 22427333
- Costa LM, Marshall E, Tesfaye M, Silverstein KA, Mori M, et al. (2014) Central cell-derived peptides regulate early embryo patterning in flowering plants. *Science* 344: 168–172. <https://doi.org/10.1126/science.1243005> PMID: 24723605
- Bayer M, Nawy T, Giglione C, Galli M, Meinel T, et al. (2009) Paternal control of embryonic patterning in Arabidopsis thaliana. *Science* 323: 1485–1488. <https://doi.org/10.1126/science.1167784> PMID: 19286558
- Pfister A, Barberon M, Alassimone J, Kalmbach L, Lee Y, et al. (2014) A receptor-like kinase mutant with absent endodermal diffusion barrier displays selective nutrient homeostasis defects. *Elife* 3: e03115. <https://doi.org/10.7554/eLife.03115> PMID: 25233277
- Xing Q, Creff A, Waters A, Tanaka H, Goodrich J, et al. (2013) ZHOUP1 controls embryonic cuticle formation via a signalling pathway involving the subtilisin protease ABNORMAL LEAF-SHAPE1 and the receptor kinases GASSHO1 and GASSHO2. *Development* 140: 770–779. <https://doi.org/10.1242/dev.088898> PMID: 23318634
- Yang S, Johnston N, Talideh E, Mitchell S, Jeffree C, et al. (2008) The endosperm-specific ZHOUP1 gene of Arabidopsis thaliana regulates endosperm breakdown and embryonic epidermal development. *Development* 135: 3501–3509. <https://doi.org/10.1242/dev.026708> PMID: 18849529
- Tsuwamoto R, Fukuoka H, Takahata Y (2008) GASSHO1 and GASSHO2 encoding a putative leucine-rich repeat transmembrane-type receptor kinase are essential for the normal development of the epidermal surface in Arabidopsis embryos. *Plant J* 54: 30–42. <https://doi.org/10.1111/j.1365-313X.2007.03395.x> PMID: 18088309
- Tanaka H, Onouchi H, Kondo M, Hara-Nishimura I, Nishimura M, et al. (2001) A subtilisin-like serine protease is required for epidermal surface formation in Arabidopsis embryos and juvenile plants. *Development* 128: 4681–4689. PMID: 11731449
- Moussu S, San-Bento R, Galletti R, Creff A, Farcot E, et al. (2013) Embryonic cuticle establishment: the great (apoplastic) divide. *Plant Signal Behav* 8: e27491. <https://doi.org/10.4161/psb.27491> PMID: 24398513
- San-Bento R, Farcot E, Galletti R, Creff A, Ingram G (2014) Epidermal identity is maintained by cell-cell communication via a universally active feedback loop in Arabidopsis thaliana. *Plant J* 77: 46–58. <https://doi.org/10.1111/tpj.12360> PMID: 24147836
- Bernard A, Joubes J (2012) Arabidopsis cuticular waxes: Advances in synthesis, export and regulation. *Prog Lipid Res* 52: 110–129. <https://doi.org/10.1016/j.plipres.2012.10.002> PMID: 23103356
- Fich EA, Segerson NA, Rose JK (2016) The Plant Polyester Cutin: Biosynthesis, Structure, and Biological Roles. *Annu Rev Plant Biol* 10.1146/annurev-arplant-043015-111929.
- Javelle M, Vernoud V, Rogowsky PM, Ingram GC (2011) Epidermis: the formation and functions of a fundamental plant tissue. *New Phytol* 189: 17–39. <https://doi.org/10.1111/j.1469-8137.2010.03514.x> PMID: 21054411
- Serrano M, Coluccia F, Torres M, L'Haridon F, Metraux JP (2014) The cuticle and plant defense to pathogens. *Front Plant Sci* 5: 274. <https://doi.org/10.3389/fpls.2014.00274> PMID: 24982666
- Tanaka T, Tanaka H, Machida C, Watanabe M, Machida Y (2004) A new method for rapid visualization of defects in leaf cuticle reveals five intrinsic patterns of surface defects in Arabidopsis. *Plant J* 37: 139–146. PMID: 14675439

18. Delude C, Moussu S, Joubes J, Ingram G, Domergue F (2016) Plant Surface Lipids and Epidermis Development. *Sub-cellular biochemistry* 86: 287–313. https://doi.org/10.1007/978-3-319-25979-6_12 PMID: 27023240
19. Le BH, Cheng C, Bui AQ, Wagmaister JA, Henry KF, et al. (2010) Global analysis of gene activity during Arabidopsis seed development and identification of seed-specific transcription factors. *Proc Natl Acad Sci U S A* 107: 8063–8070. <https://doi.org/10.1073/pnas.1003530107> PMID: 20385809
20. Winter D, Vinegar B, Nahal H, Ammar R, Wilson GV, et al. (2007) An "Electronic Fluorescent Pictograph" browser for exploring and analyzing large-scale biological data sets. *PLoS One* 2: e718. <https://doi.org/10.1371/journal.pone.0000718> PMID: 17684564
21. Belmonte MF, Kirkbride RC, Stone SL, Pelletier JM, Bui AQ, et al. (2013) Comprehensive developmental profiles of gene activity in regions and subregions of the Arabidopsis seed. *Proc Natl Acad Sci U S A* 110: E435–444. <https://doi.org/10.1073/pnas.1222061110> PMID: 23319655
22. Lu S, Song T, Kosma DK, Parsons EP, Rowland O, et al. (2009) Arabidopsis CER8 encodes LONG-CHAIN ACYL-COA SYNTHETASE 1 (LACS1) that has overlapping functions with LACS2 in plant wax and cutin synthesis. *Plant J* 59: 553–564. <https://doi.org/10.1111/j.1365-313X.2009.03892.x> PMID: 19392700
23. Schnurr J, Shockey J, Browse J (2004) The acyl-CoA synthetase encoded by LACS2 is essential for normal cuticle development in Arabidopsis. *Plant Cell* 16: 629–642. <https://doi.org/10.1105/tpc.017600> PMID: 14973169
24. Li-Beisson Y, Shorrosh B, Beisson F, Andersson MX, Arondel V, et al. (2013) Acyl-lipid metabolism. *Arabidopsis Book* 11: e0161. <https://doi.org/10.1199/tab.0161> PMID: 23505340
25. Beisson F, Li-Beisson Y, Pollard M (2012) Solving the puzzles of cutin and suberin polymer biosynthesis. *Curr Opin Plant Biol* 15: 329–337. <https://doi.org/10.1016/j.pbi.2012.03.003> PMID: 22465132
26. Pruitt RE, Vielle-Calzada JP, Ploense SE, Grossniklaus U, Lolle SJ (2000) FIDDLEHEAD, a gene required to suppress epidermal cell interactions in Arabidopsis, encodes a putative lipid biosynthetic enzyme. *Proc Natl Acad Sci U S A* 97: 1311–1316. PMID: 10655527
27. Yephremov A, Wisman E, Huijser P, Huijser C, Wellesen K, et al. (1999) Characterization of the FIDDLEHEAD gene of Arabidopsis reveals a link between adhesion response and cell differentiation in the epidermis. *The Plant Cell* 11: 2187–2201. PMID: 10559443
28. Wellesen K, Durst F, Pinot F, Benveniste I, Nettesheim K, et al. (2001) Functional analysis of the LACERATA gene of Arabidopsis provides evidence for different roles of fatty acid omega-hydroxylation in development. *Proc Natl Acad Sci U S A* 98: 9694–9699. <https://doi.org/10.1073/pnas.171285998> PMID: 11493698
29. Kurdyukov S, Faust A, Nawrath C, Bar S, Voisin D, et al. (2006) The epidermis-specific extracellular BODYGUARD controls cuticle development and morphogenesis in Arabidopsis. *Plant Cell* 18: 321–339. <https://doi.org/10.1105/tpc.105.036079> PMID: 16415209
30. Debono A, Yeats TH, Rose JK, Bird D, Jetter R, et al. (2009) Arabidopsis LTPG Is a Glycosylphosphatidylinositol-Anchored Lipid Transfer Protein Required for Export of Lipids to the Plant Surface. *Plant Cell*.
31. Bird D, Beisson F, Brigham A, Shin J, Greer S, et al. (2007) Characterization of Arabidopsis ABCG11/WBC11, an ATP binding cassette (ABC) transporter that is required for cuticular lipid secretion. *Plant J* 52: 485–498. <https://doi.org/10.1111/j.1365-313X.2007.03252.x> PMID: 17727615
32. Li Y, Beisson F, Koo AJ, Molina I, Pollard M, et al. (2007) Identification of acyltransferases required for cutin biosynthesis and production of cutin with suberin-like monomers. *Proc Natl Acad Sci U S A* 104: 18339–18344. <https://doi.org/10.1073/pnas.0706984104> PMID: 17991776
33. Sarnowski TJ, Rios G, Jasik J, Swiezewski S, Kaczanowski S, et al. (2005) SWI3 subunits of putative SWI/SNF chromatin-remodeling complexes play distinct roles during Arabidopsis development. *Plant Cell* 17: 2454–2472. <https://doi.org/10.1105/tpc.105.031203> PMID: 16055636
34. Shiu SH, Bleecker AB (2001) Receptor-like kinases from Arabidopsis form a monophyletic gene family related to animal receptor kinases. *Proc Natl Acad Sci U S A* 98: 10763–10768. <https://doi.org/10.1073/pnas.181141598> PMID: 11526204
35. Shiu SH, Bleecker AB (2003) Expansion of the receptor-like kinase/Pelle gene family and receptor-like proteins in Arabidopsis. *Plant Physiol* 132: 530–543. <https://doi.org/10.1104/pp.103.021964> PMID: 12805585
36. Yamaguchi Y, Huffaker A, Bryan AC, Tax FE, Ryan CA (2010) PEPR2 is a second receptor for the Pep1 and Pep2 peptides and contributes to defense responses in Arabidopsis. *Plant Cell* 22: 508–522. <https://doi.org/10.1105/tpc.109.068874> PMID: 20179141

37. Krol E, Mentzel T, Chinchilla D, Boller T, Felix G, et al. (2010) Perception of the Arabidopsis danger signal peptide 1 involves the pattern recognition receptor AtPEPR1 and its close homologue AtPEPR2. *J Biol Chem* 285: 13471–13479. <https://doi.org/10.1074/jbc.M109.097394> PMID: 20200150
38. Yamaguchi Y, Huffaker A (2011) Endogenous peptide elicitors in higher plants. *Curr Opin Plant Biol* 14: 351–357. <https://doi.org/10.1016/j.pbi.2011.05.001> PMID: 21636314
39. Lopez-Bucio JS, Dubrovsky JG, Raya-Gonzalez J, Ugartechea-Chirino Y, Lopez-Bucio J, et al. (2014) Arabidopsis thaliana mitogen-activated protein kinase 6 is involved in seed formation and modulation of primary and lateral root development. *J Exp Bot* 65: 169–183. <https://doi.org/10.1093/jxb/ert368> PMID: 24218326
40. Zhang M, Wu H, Su J, Wang H, Zhu Q, et al. (2017) Maternal control of embryogenesis by MPK6 and its upstream MKK4/MKK5 in Arabidopsis. *Plant J* 92: 1005–1019. <https://doi.org/10.1111/tpj.13737> PMID: 29024034
41. Moussu S, Doll NM, Chamot S, Brocard L, Creff A, et al. (2017) ZHOUP1 and KERBEROS Mediate Embryo/Endosperm Separation by Promoting the Formation of an Extracuticular Sheath at the Embryo Surface. *Plant Cell* 29: 1642–1656. <https://doi.org/10.1105/tpc.17.00016> PMID: 28696222
42. Zhang Y, Wang P, Shao W, Zhu JK, Dong J (2015) The BASL polarity protein controls a MAPK signaling feedback loop in asymmetric cell division. *Dev Cell* 33: 136–149. <https://doi.org/10.1016/j.devcel.2015.02.022> PMID: 25843888
43. Sethi V, Raghuram B, Sinha AK, Chattopadhyay S (2014) A mitogen-activated protein kinase cascade module, MKK3-MPK6 and MYC2, is involved in blue light-mediated seedling development in Arabidopsis. *Plant Cell* 26: 3343–3357. <https://doi.org/10.1105/tpc.114.128702> PMID: 25139007
44. Smekalova V, Luptovciak I, Komis G, Samajova O, Ovecka M, et al. (2014) Involvement of YODA and mitogen activated protein kinase 6 in Arabidopsis post-embryonic root development through auxin up-regulation and cell division plane orientation. *New Phytol* 203: 1175–1193. <https://doi.org/10.1111/nph.12880> PMID: 24923680
45. Guan Y, Meng X, Khanna R, LaMontagne E, Liu Y, et al. (2014) Phosphorylation of a WRKY transcription factor by MAPKs is required for pollen development and function in Arabidopsis. *PLoS Genet* 10: e1004384. <https://doi.org/10.1371/journal.pgen.1004384> PMID: 24830428
46. Guan Y, Lu J, Xu J, McClure B, Zhang S (2014) Two Mitogen-Activated Protein Kinases, MPK3 and MPK6, Are Required for Funicular Guidance of Pollen Tubes in Arabidopsis. *Plant Physiol* 165: 528–533. <https://doi.org/10.1104/pp.113.231274> PMID: 24717717
47. Jewaria PK, Hara T, Tanaka H, Kondo T, Betsuyaku S, et al. (2013) Differential effects of the peptides Stomagen, EPF1 and EPF2 on activation of MAP kinase MPK6 and the SPCH protein level. *Plant Cell Physiol* 54: 1253–1262. <https://doi.org/10.1093/pcp/pct076> PMID: 23686240
48. Khan M, Rozhon W, Bigeard J, Pflieger D, Husar S, et al. (2013) Brassinosteroid-regulated GSK3/Shaggy-like kinases phosphorylate mitogen-activated protein (MAP) kinase kinases, which control stomata development in Arabidopsis thaliana. *J Biol Chem* 288: 7519–7527. <https://doi.org/10.1074/jbc.M112.384453> PMID: 23341468
49. Meng X, Wang H, He Y, Liu Y, Walker JC, et al. (2012) A MAPK cascade downstream of ERECTA receptor-like protein kinase regulates Arabidopsis inflorescence architecture by promoting localized cell proliferation. *Plant Cell* 24: 4948–4960. <https://doi.org/10.1105/tpc.112.104695> PMID: 23263767
50. Muller J, Beck M, Mettlich U, Komis G, Hause G, et al. (2010) Arabidopsis MPK6 is involved in cell division plane control during early root development, and localizes to the pre-prophase band, phragmoplast, trans-Golgi network and plasma membrane. *Plant J* 61: 234–248. <https://doi.org/10.1111/j.1365-3113.2009.04046.x> PMID: 19832943
51. Cho SK, Larue CT, Chevalier D, Wang H, Jinn TL, et al. (2008) Regulation of floral organ abscission in Arabidopsis thaliana. *Proc Natl Acad Sci U S A* 105: 15629–15634. <https://doi.org/10.1073/pnas.0805539105> PMID: 18809915
52. Wang H, Liu Y, Bruffett K, Lee J, Hause G, et al. (2008) Haplo-insufficiency of MPK3 in MPK6 mutant background uncovers a novel function of these two MAPKs in Arabidopsis ovule development. *Plant Cell* 20: 602–613. <https://doi.org/10.1105/tpc.108.058032> PMID: 18364464
53. Ren D, Liu Y, Yang KY, Han L, Mao G, et al. (2008) A fungal-responsive MAPK cascade regulates phytoalexin biosynthesis in Arabidopsis. *Proc Natl Acad Sci U S A* 105: 5638–5643. <https://doi.org/10.1073/pnas.0711301105> PMID: 18378893
54. Moussu SA, Doll NM, Chamot S, Brocard L, Creff A, et al. (2017) ZHOUP1 and KERBEROS Mediate Embryo/Endosperm Separation by Promoting the Formation of an Extra-Cuticular Sheath at the Embryo Surface. *Plant Cell* 10.1105/tpc.17.00016.
55. Denay G, Creff A, Moussu S, Wagnon P, Thevenin J, et al. (2014) Endosperm breakdown in Arabidopsis requires heterodimers of the basic helix-loop-helix proteins ZHOUP1 and INDUCER OF CBP EXPRESSION 1. *Development* 141: 1222–1227. <https://doi.org/10.1242/dev.103531> PMID: 24553285

56. Bartels S, Lori M, Mbengue M, van Verk M, Klauser D, et al. (2013) The family of Peps and their precursors in Arabidopsis: differential expression and localization but similar induction of pattern-triggered immune responses. *J Exp Bot* 64: 5309–5321. <https://doi.org/10.1093/jxb/ert330> PMID: 24151300
57. Postel S, Kufner I, Beuter C, Mazzotta S, Schwedt A, et al. (2010) The multifunctional leucine-rich repeat receptor kinase BAK1 is implicated in Arabidopsis development and immunity. *Eur J Cell Biol* 89: 169–174. <https://doi.org/10.1016/j.ejcb.2009.11.001> PMID: 20018402
58. Kim BH, Kim SY, Nam KH (2013) Assessing the diverse functions of BAK1 and its homologs in Arabidopsis, beyond BR signaling and PTI responses. *Molecules and cells* 35: 7–16. <https://doi.org/10.1007/s10059-013-2255-3> PMID: 23269431
59. Lee Y, Rubio MC, Alassimone J, Geldner N (2013) A mechanism for localized lignin deposition in the endodermis. *Cell* 153: 402–412. <https://doi.org/10.1016/j.cell.2013.02.045> PMID: 23541512
60. Steinhorst L, Kudla J (2013) Calcium and reactive oxygen species rule the waves of signaling. *Plant Physiol* 163: 471–485. <https://doi.org/10.1104/pp.113.222950> PMID: 23898042
61. Kadota Y, Shirasu K, Zipfel C (2015) Regulation of the NADPH Oxidase RBOHD During Plant Immunity. *Plant Cell Physiol* 56: 1472–1480. <https://doi.org/10.1093/pccp/pcv063> PMID: 25941234
62. Dominguez E, Heredia-Guerrero JA, Heredia A (2015) Plant cutin genesis: unanswered questions. *Trends Plant Sci* 20: 551–558. <https://doi.org/10.1016/j.tplants.2015.05.009> PMID: 26115781
63. Liu Y, He C (2017) A review of redox signaling and the control of MAP kinase pathway in plants. *Redox Biol* 11: 192–204. <https://doi.org/10.1016/j.redox.2016.12.009> PMID: 27984790
64. Jalmi SK, Sinha AK (2015) ROS mediated MAPK signaling in abiotic and biotic stress- striking similarities and differences. *Front Plant Sci* 6: 769. <https://doi.org/10.3389/fpls.2015.00769> PMID: 26442079
65. Ellinger D, Voigt CA (2014) Callose biosynthesis in Arabidopsis with a focus on pathogen response: what we have learned within the last decade. *Annals of botany* 114: 1349–1358. <https://doi.org/10.1093/aob/mcu120> PMID: 24984713
66. Voigt CA (2014) Callose-mediated resistance to pathogenic intruders in plant defense-related papillae. *Front Plant Sci* 5: 168. <https://doi.org/10.3389/fpls.2014.00168> PMID: 24808903
67. Tang D, Simonich MT, Innes RW (2007) Mutations in LACS2, a long-chain acyl-coenzyme A synthetase, enhance susceptibility to avirulent *Pseudomonas syringae* but confer resistance to *Botrytis cinerea* in Arabidopsis. *Plant Physiology* 144: 1093–1103. <https://doi.org/10.1104/pp.106.094318> PMID: 17434992
68. Xiao F, Goodwin SM, Xiao Y, Sun Z, Baker D, et al. (2004) Arabidopsis CYP86A2 represses *Pseudomonas syringae* type III genes and is required for cuticle development. *EMBO J* 23: 2903–2913. <https://doi.org/10.1038/sj.emboj.7600290> PMID: 15241470
69. Waters A, Creff A, Goodrich J, Ingram G (2013) "What we've got here is failure to communicate": Zou mutants and endosperm cell death in seed development. *Plant Signal Behav* 8.
70. Pearce G, Yamaguchi Y, Barona G, Ryan CA (2010) A subtilisin-like protein from soybean contains an embedded, cryptic signal that activates defense-related genes. *Proc Natl Acad Sci U S A* 107: 14921–14925. <https://doi.org/10.1073/pnas.1007568107> PMID: 20679205
71. Ramirez V, Lopez A, Mauch-Mani B, Gil MJ, Vera P (2013) An extracellular subtilase switch for immune priming in Arabidopsis. *PLoS Pathog* 9: e1003445. <https://doi.org/10.1371/journal.ppat.1003445> PMID: 23818851
72. Nakayama T, Shinohara H, Tanaka M, Baba K, Ogawa-Ohnishi M, et al. (2017) A peptide hormone required for Casparian strip diffusion barrier formation in Arabidopsis roots. *Science* 355: 284–286. <https://doi.org/10.1126/science.aai9057> PMID: 28104889
73. Doblaz VG, Smakowska-Luzan E, Fujita S, Alassimone J, Barberon M, et al. (2017) Root diffusion barrier control by a vasculature-derived peptide binding to the SGN3 receptor. *Science* 355: 280–284. <https://doi.org/10.1126/science.aaj1562> PMID: 28104888
74. Ursache R, Andersen TG, Marhavý P, Geldner N (2018) A protocol for combining fluorescent proteins with histological stains for diverse cell wall components. *Plant J* 93:399–412. <https://doi.org/10.1111/tpj.13784> PMID: 29171896
75. Domergue F, Vishwanath SJ, Joubes J, Ono J, Lee JA, et al. (2010) Three Arabidopsis fatty acyl-coenzyme A reductases, FAR1, FAR4, and FAR5, generate primary fatty alcohols associated with suberin deposition. *Plant Physiol* 153: 1539–1554. <https://doi.org/10.1104/pp.110.158238> PMID: 20571114
76. Bourdenx B, Bernard A, Domergue F, Pascal S, Leger A, et al. (2011) Overexpression of Arabidopsis ECERIFERUM1 promotes wax very-long-chain alkane biosynthesis and influences plant response to biotic and abiotic stresses. *Plant Physiol* 156: 29–45. <https://doi.org/10.1104/pp.111.172320> PMID: 21386033

77. Gagnet S, Tamby JP, Martin-Magniette ML, Bitton F, Taconnat L, et al. (2008) CATdb: a public access to Arabidopsis transcriptome data from the URGV-CATMA platform. *Nucleic Acids Res* 36: D986–990. <https://doi.org/10.1093/nar/gkm757> PMID: 17940091
78. Derozier S, Samson F, Tamby JP, Guichard C, Brunaud V, et al. (2011) Exploration of plant genomes in the FLAGdb++ environment. *Plant Methods* 7: 8. <https://doi.org/10.1186/1746-4811-7-8> PMID: 21447150
79. Yang YH, Dudoit S, Luu P, Lin DM, Peng V, et al. (2002) Normalization for cDNA microarray data: a robust composite method addressing single and multiple slide systematic variation. *Nucleic Acids Res* 30: e15. PMID: 11842121
80. Smyth GK (2004) Linear models and empirical bayes methods for assessing differential expression in microarray experiments. *Statistical applications in genetics and molecular biology* 3: Article3.
81. Storey JD, Tibshirani R (2003) Statistical significance for genomewide studies. *Proc Natl Acad Sci U S A* 100: 9440–9445. <https://doi.org/10.1073/pnas.1530509100> PMID: 12883005